

GEOMORPHOLOGY AT THE CONFLUENCE  
OF STREAM RESTORATION AND FLOOD CONTROL

A Thesis submitted to the faculty of  
San Francisco State University  
In partial fulfillment of  
the requirements for  
the Degree

Master of Arts

In

Geography: Resource Management and Environmental Planning

by

Genevieve Munsey

San Francisco, California

May 2015

Copyright by  
Genevieve Munsey  
2015

## CERTIFICATION OF APPROVAL

I certify that I have read *Geomorphology at the Confluence of Stream Restoration and Flood Control* by Genevieve Munsey, and that in my opinion this work meets the criteria for approving a thesis submitted in partial fulfillment of the requirement for the degree Master of Arts in Geography: Resource Management and Environmental Planning at San Francisco State University.

---

Jerry Davis, Ph.D.  
Professor

---

Leonhard Blesius, Ph.D.  
Associate Professor

GEOMORPHOLOGY AT THE CONFLUENCE  
OF STREAM RESTORATION AND FLOOD CONTROL

Genevieve Munsey  
San Francisco, California  
2015

This study assesses the geomorphologic response of a stream management project integrating ecological restoration principles with flood control. Damaging floods on the coastal stream San Pedro Creek in Pacifica, California, led to replacement of the straightened and incised natural channel with a constructed meander and vegetated floodplain. The intention was to mitigate flooding and increase habitat for species such as the federally-listed threatened Central California steelhead (*Oncorhynchus mykiss*). Longitudinal profile data show a degradation and aggradation oscillation. Smaller scale meanders have begun to form on the straight reaches between larger designed meanders. Headcutting backwaters at an inflection point initiated a chute cut-off. Preliminary flood modeling demonstrates less than a 50-year flood protection level. These results suggest that the stream reach is not stabilizing as designed, but is instead adjusting according to geomorphological principles. Specifically, the radius of curvature and the meander wavelength are decreasing. Further research is needed to understand lateral controls and the chute cut-off process in small urban stream restoration and flood control projects.

I certify that the **ABSTRACT** is a correct representation of the content of this thesis.

---

Chair, Thesis Committee

---

Date

## TABLE OF CONTENTS

List of Tables .....	vii
List of Figures .....	viii
Introduction.....	1
Study Area .....	4
Historical land use.....	4
San Pedro Creek as flood hazard.....	6
Climate .....	7
Geology .....	8
San Pedro Creek as habitat.....	11
Restoration and flood control.....	14
SPC channel design theoretical values.....	14
Flood capacity modeling and USACE design variables .....	19
Daily precipitation data, discharge, and return intervals.....	23
SPC restoration installation.....	25
Meander and channel adjustment theory.....	28
Methods.....	32
Fieldwork .....	32
Remote sensing and planview measurements .....	33
USACE documents and the HEC-RAS model.....	33
Documentary photography .....	35

Daily precipitation data .....	35
Results.....	36
Vegetation observations .....	36
Precipitation and flooding.....	37
Remote sensing and planviews .....	43
Meander planform variables.....	46
Longitudinal profiles and cross-sections.....	49
HEC-RAS flood model .....	57
Meander adjustments.....	59
Point bars.....	59
Secondary channel formation and chute cut-off .....	62
Lateral control adjustments .....	68
Culverts .....	71
The trajectory of a dislodged log revetment.....	75
Anthropogenic influences .....	83
Discussion.....	87
Longitudinal profiles, cross-sections, and lateral controls.....	87
Restoration design and meander adjustments .....	88
Flood model.....	90
Considerations for future research .....	91
Conclusions.....	93
References.....	96

## LIST OF TABLES

Table 1: SPC FCP restoration theoretical values .....	17
Table 2: Calculated precipitation for various return intervals .....	41
Table 3: Calculated return intervals for the storms in 1982, 2005, and 2008.....	41
Table 4: SPC FCP bedform and floodplain variable comparison.....	48

## LIST OF FIGURES

Figure 1: The stream study area overlays an 1866 T-sheet .....	5
Figure 2: The study area in 2005 .....	6
Figure 3: Climograph for Pacifica, California .....	7
Figure 4: Annual precipitation 1950–2013 .....	8
Figure 5: Geology of lower San Francisco peninsula and San Mateo County .....	9
Figure 6: Geology of San Pedro Creek watershed.....	10
Figure 7: California red-legged frog on SPC .....	12
Figure 8: Steelhead fingerling.....	13
Figure 9: Bankfull dimensions by drainage area .....	15
Figure 10: Discharge and water surface elevation.....	22
Figure 11: Model variables upstream of Highway 1 .....	23
Figure 12: Model variables near cross-section 2 (CS2/X-S2) .....	23
Figure 13: High resolution LiDAR .....	34
Figure 14: Precipitation data station locations.....	37
Figure 15: Daily rainfall 1978–2012.....	38
Figure 16: Correlating annual precipitation at SFO and SPVP .....	39
Figure 17: Annual maximum daily precipitation return intervals .....	39
Figure 18: Precipitation return interval trendlines .....	41
Figure 19: San Gregorio Creek discharge and precipitation correlation .....	43
Figure 20 (previous page): USGS high-resolution aerial orthoimagery.....	45
Figure 21: Planviews comparing LiDAR and other data sources.....	46
Figure 22: Concavity changes.....	47
Figure 23: Planview sketch and locations of photographs (“A”, “B”, “C”, etc.) .....	49
Figure 24: Longitudinal profile comparison I.....	50
Figure 25: Longitudinal profile comparison II .....	50
Figure 26: Cross-section 1 (CS1).....	52
Figure 27: Cross-section 2 (CS2).....	53
Figure 28: Either bedrock or erosion-resistant Quaternary clays .....	53
Figure 29: Cross-section 3 (CS3).....	55
Figure 30: Pebble counts for 2007 .....	56
Figure 31: Pebble counts for 2011 .....	56
Figure 32: HEC-RAS model result for 100-year flood.....	58

Figure 33: 2013 photo looking upstream towards CS2 .....	60
Figure 34: 2004 same view of CS2.....	60
Figure 35: 2011 mid-channel bar with split thalweg at photo location "E".....	61
Figure 36: 2014 repeat photograph of location "E".....	61
Figure 37: 2013 meander form with muddy banks looking upstream from location "I" .	62
Figure 38: 2007 backwater eddy and headcut located at "A".....	63
Figure 39: 2011 Repeat photography of location "A".....	64
Figure 40: 2013 Repeat photography of location "A" .....	64
Figure 41: Upstream of "A" at location "B" in 2007.....	65
Figure 42: Looking across to the left bank from the channel at "B" in 2007 .....	66
Figure 43: 2013 photo looking upstream from location "B" showing chute cut-off .....	67
Figure 44: 2008 repeat photograph from location "B" .....	67
Figure 45: Log revetments and vertical logs merged into the right bank at location "B"	69
Figure 46: Rootwad back up behind a point bar at location "C" .....	69
Figure 47: 2013 rootwad at location "H" indicates the original left bank .....	70
Figure 48: Mid-2014 rootwad at location "H" .....	70
Figure 49: Late-2014 rootwad (middle background) at location "H", during a flood.....	71
Figure 50: "Culvert 1" drains under the decommissioned road.....	72
Figure 51: Looking up the ditch that drains from "culvert 1" .....	72
Figure 52: The ditch draining "culvert 1" .....	73
Figure 53: A second culvert, "culvert 2" .....	74
Figure 54: A third pipe, "culvert 3" .....	74
Figure 55: A cobble and pebble bar in early 2013 at location "F" .....	76
Figure 56: August 2014 point bar at location "F".....	76
Figure 57: March 2013 point bar at location "F".....	77
Figure 58: December 2014 point bar at location "F" recruits a large blown out log.....	77
Figure 59: 2007 blown log revetment at location "G" .....	79
Figure 60: Blown out revetment at "G" opened up downstream by 2011 .....	79
Figure 61: Early 2008 flood event shows the blown revetment at location "G" .....	80
Figure 62: Looking downstream at the revetment at location "G" in 2011 .....	80
Figure 63: Late 2014 flood event shows the blown out log revetment at location "F" ....	81
Figure 64: Hypothesis for the log movement (brown) and culvert flow .....	82
Figure 65: 2008 peak flood event, looking downstream at the Highway 1 Bridge .....	83
Figure 66: Looking downstream at the Highway 1 Bridge in 2013 .....	84
Figure 67: The Highway 1 Bridge was .....	84
Figure 68: Homeowner landscaping with Juncus along the easement terrace at CS2.....	85
Figure 69: Homeless encampment near CS1 .....	86

## INTRODUCTION

Flood control has one clear goal: reduction of the hazards of peak flows to human populations and infrastructure. Restoration, on the other hand, may have goals such as riparian and aquatic habitat enhancement, dam removal for naturalization of flow regimes and sediment supply, improvement of water quality, re-establishment of connectivity to flood plains, or beautification (Kondolf 1998, Kondolf et al. 2007, Wilcock 2012). Though flood control and ecological stream restoration are both human interventions with nature, they descend from very different ideological and bureaucratic lineages in the United States. Flood control is largely the domain of engineers, and in many cases is managed by the United States Army Corps of Engineers (USACE), while stream restoration comes from restoration ecology and fluvial geomorphology theory. In practice, stream restoration plans often come from designers who are neither ecologists nor geomorphologists (Kondolf 1998, Wilcock 2012), much less both.

Following long-term modifications of waterways for first European-style agriculture and then expanding urbanization, the floodplain reach of San Pedro Creek (SPC) in Pacifica, California was left a narrow confined channel, albeit vegetated and dirt-lined. Subsequently, flashier hydrograph storm response times (Amato 2003), compromised water quality (Davis et al. 2004, Ivanetich et al. 2006), and inadequate aquatic salmonid habitat (Johnson 2005) added to the serious hazard of repeat flooding of business and residential areas north of the downstream floodplain reach (McDonald 2004).

With the onset of the environmental movement in the 1960s, a series of new federal laws were passed that required federal agencies to consider and mitigate the environmental impacts of human activities. The National Environmental Policy Act (NEPA), enacted in 1970, prioritized environmental protection and required that federal agencies prepare Environmental Impact Statements (EIS) for new projects, which would be open to public

comment (Wagner 1976). USACE, the federal agency responsible for flood control in the United States, became subject to NEPA and EIS just as it began working with the City of Pacifica (CP), California on their flooding problems. In 1973 and 1974, Wagner (1976) applied the practice of public participation in USACE's flood protection process to the test case of flooding in Pacifica. He concluded that some USACE personnel were "less than enthusiastic" about collaborating with the public and researchers, and could benefit from formal training in working in interdisciplinary planning groups (Wagner 1976, p. 228 and p. 244).

The planning took another 25 years, during which time the environmental movement grew, eventually resulting in an effective alignment of public officials both locally and federally who were on board with ecological restoration goals for SPC (McDonald 2004). Flood protection options progressed from hard-path solutions such as higher flood walls along the linear natural channel, with an overflow doubling as a recreational area, to softer-path solutions including a stream meander, rootwad and footer log revetments, floodplain connectivity, and native revegetation (CP and USACE 1998). This followed the general trend in stream restoration in California (Kondolf et al. 2007).

Wilcock (2012) criticizes the stream management practice of fixing channel geometry with rip-rap and other softer (but still hard) path solutions because it prevents a natural, dynamic channel. However, these design elements qualify for restoration projects requiring Rosgen-style natural channel design described in Rosgen (1994). Wilcock (2012) similarly disapproves of floodplain connectivity projects that anchor a too-small channel with hardspots in order to encourage more regular overbank flow.

This case study investigates the geomorphologic consequences of integrating ecological stream restoration principles into a federal flood control project on San Pedro Creek. Research objectives include assessing the stability of the stream reach, comparing

planning and design variables with outcomes, and investigating meander adjustments in a laterally controlled reach. Using field survey data, high-resolution LiDAR data, and documentary photography, this study investigates the geomorphology of the San Pedro Creek flood control project restoration reach ten years after its installation. System stability assessment is based on longitudinal profiles, cross-sections, planviews, and process analysis, with a particular focus on the meander process in a laterally controlled stream restoration system. Finally, estimates of the flood protection achieved are posited alongside suggestions for further study.

## STUDY AREA

### **Historical land use**

San Pedro Creek drains a 21 km<sup>2</sup> watershed in Pacifica, 24 km south of San Francisco along the California coast. Prior to Spanish colonization of the area in the late 1700s, the creek drained into a large wetland, willow grove, and lake before opening to the Pacific Ocean (Culp 2002) (Figure 1). The Costanoan Ohlone had maintained grasslands in the area through controlled burning (Davis et al. 2004). The Costanoans and Spaniards then grazed cattle for the San Francisco Mission, channelizing and draining parts of the wetland and lake. Later, Mexican and then American settlers, along with Costanoans defrauded of land ownership, but remaining as hired hands, used this area for ranching and farming the valley bottom. This left the creek ditched and straightened by 1896 and the lake and wetlands drained or diverted completely by 1915 (Culp 2002).

The valley is surrounded by steep slopes affected by gullying and landslides largely due to local anthropogenic land use practices (Davis et al. 2004). Cattle grazing and other agricultural activities initiated the gullying, which is still problematic today, and compacted soils, which increased overland flow. Additionally, land use practices in the South and Middle Forks accelerated erosion of fine sediments (Collins 2001, Davis et al. 2004, Davis and Sims 2013). More recently, starting in the 1950s, urban development increased impervious surfaces and culverted most of the North Fork tributary, thereby increasing the drainage density, decreasing lag time to peak flow during storm events, and increasing maximum discharge volume and instream erosion (Amato 2003, Davis et al. 2004). The culverts also decreased sediment supply from the North Fork to the mainstem (Pearce, McKee, & Shonkoff 2004).

The 4.3 km mainstem of the creek drains to the northwest through the urbanized valley and into the Pacific Ocean. Today, the eastern and southern tributaries of the watershed

are largely parklands managed by county, state, and federal agencies; approximately two thirds of the watershed are in natural protected areas. Native coastal scrub, mainly below 150 m elevation, and native chaparral above 150 m are both dominated by shrubs. Introduced eucalyptus groves (*Eucalyptus globulus*), as well as introduced Monterey pine (*Pinus radiata*) and Monterey cypress (*Cupressus macrocarpa*) stands, are found on the lower southern slopes of the watershed (Amato 2003). These shrub and forest assemblages dominate the undeveloped areas, where neither Ohlone fires, nor grazing cattle, maintain the former grasslands (Collins 2001). Native grasses and exotic introduced European grasses persist on some northern ridges and low-lying natural and riparian areas of the watershed (SPCWC 2002, Amato 2003).

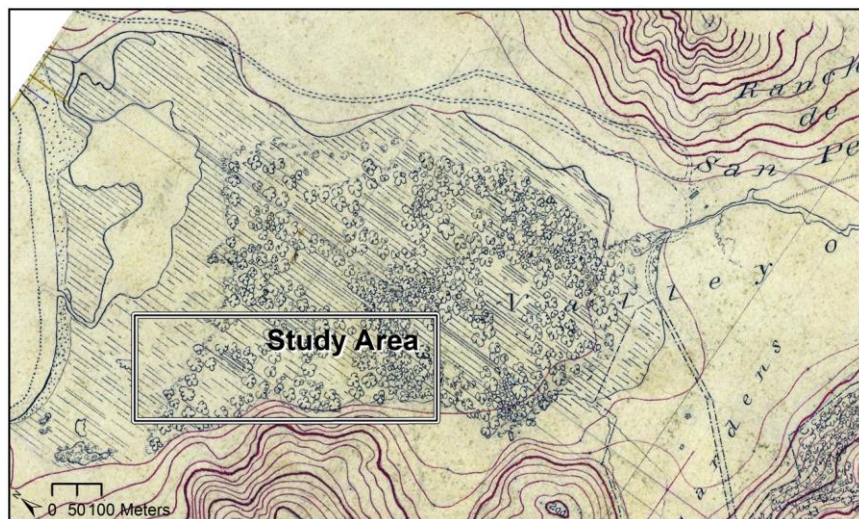


Figure 1: The stream study area overlays an 1866 T-sheet. By 1896 the stream was straightened and by 1915 the willow grove and wetland area were drained (Culp 2002).

The 1866 T-sheet (T01019-00) is a topographic shoreline map produced by the National Ocean Survey (Figure 1). It shows that virtually the entire 0.8 km<sup>2</sup> valley area below 6 m elevation was drawn as a wetland, including a small lake (< 0.1 km<sup>2</sup>) and a large riparian forest likely of willows (0.4 km<sup>2</sup>). Eighty percent of the study area reach is within this historic willow patch, or sausal. However, the restoration wetland floodplain is less than

0.04 km<sup>2</sup>. The remainder of the historic wetland and lake are now business and residential areas (Figure 2).



Figure 2: The study area in 2005. Shopping and residential areas are to the north and the creek passes beneath Highway 1 before draining into the Pacific Ocean.

### **San Pedro Creek as flood hazard**

Following urbanization, there were floods in 1956, 1958, and then a larger flood in 1962. The City of Pacifica had to remove debris trapped behind the Highway 1 Bridge crossing because it contributed to the flooding. Floods again in 1972, 1976, and 1982, tormented the town with repeated flood damage to the business district and residential areas directly adjacent north of the stream and east of Highway 1 (Culp 2002).

The approximately 800 m long lowermost stream area qualifies for federal flood protection assistance as a Section 205 area, which allows federal funding for small flood control projects (Small Flood Control Project Authority 1976). The 500 m long area just upstream of Highway 1 is the flood control project (FCP), which is the study area for this investigation (Figure 2). In the 1970s, the San Francisco office of USACE began the conversation about flood control in Pacifica. The study area eventually underwent a restoration from 2000–2004 (Wagner 1976, Collins 2001, McDonald 2004).

## Climate

Pacifica has a Mediterranean climate with cool foggy summers and mild wet winters.

Precipitation is exclusively rainfall and occurs in the winter months (Figure 3).

Precipitation averages 956 mm per year in the area, much higher than the 507 mm for San Francisco Airport (SFO), which is also on the San Francisco peninsula, to the east on the leeward side over a ridge. Amato (2003) found the San Pedro Valley Park (SPVP) precipitation data to be an average between two tip bucket gauges installed in the watershed and suggested it may be a proxy for San Pedro Watershed precipitation generally. Annual precipitations values were available at SPVP for the fiscal years, July to June, from 1981 to present. They are presented alongside precipitation at SFO for 1950 to present and SPVP estimated values for 1950 to 1980 (Figure 4). Significant flood event years are also indicated on the graph. Temperatures on the peninsula range from 10° to 20° Celsius, averaging 14° (Figure 3).

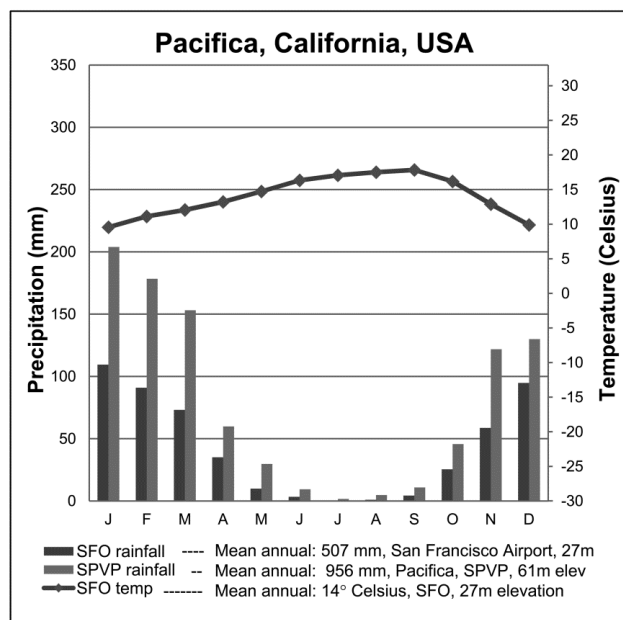


Figure 3: Climograph for Pacifica, California. Data courtesy of San Pedro Valley Park and wrcc.dri.edu.

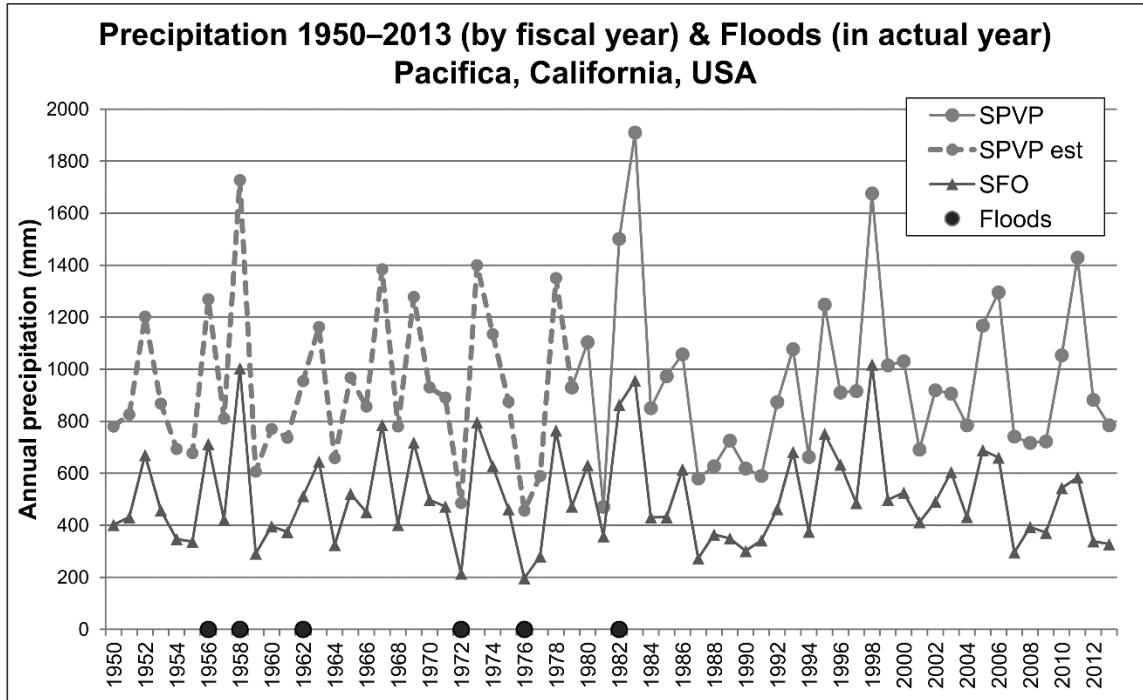


Figure 4: Annual precipitation 1950–2013. Dashed SPVP value calculation described in the Results Section. (Data courtesy of San Pedro Valley Park and wrcc.dri.edu.)

## Geology

California coastal mountains have been produced in part by local compression along the meeting of the North American Plate and the Pacific Plate where the right-lateral slip fault has nonlinear bends (Stoffer 2006). The San Pedro Valley itself is produced by a combination of the compression within the complex San Andres Fault zone (Figure 5), the NW trending ravines produced by the slip, and the slip preventing headwater growth of the watershed (Stoffer 2006). Due to their tectonic situation, the small coastal watersheds in this area have experienced uplift and as a result, have steeply eroding upper reaches with a propensity for landslides (Brabb, Pampeyan, & Bonilla 1972; Davis and Sims 2013). The sharp incline to the south of the San Pedro Creek study area reach is an example of this steep incline, with a slope of 35% rising quickly to 180 m elevation in a 0.4 km<sup>2</sup> subwatershed in Pedro Point Headlands (see Figure 1, where contour lines show this steep rise to the south of the study area).

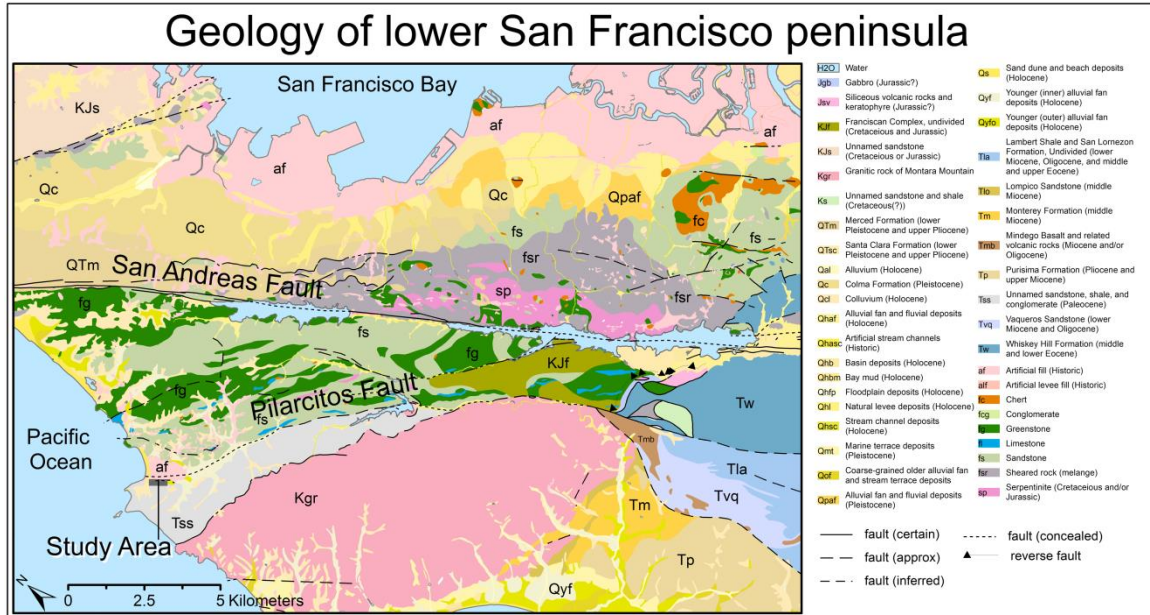


Figure 5: Geology of lower San Francisco peninsula and San Mateo County. Modified from Brabb, Graymer, & Jones (1998). Please see original map for the details of geological units.

The San Pedro Creek Watershed valley bottom is defined by inactive fault lines, including one unnamed fault near the study reach (Figure 6 inset). The Pilarcitos Fault runs parallel just north of the study area. It was confirmed to be an inactive segment of the San Andreas Fault system, which is currently located 8 km to the northeast (Parsons et al. 2002).

The right-lateral San Andreas Fault system replaced a subduction zone 28 m.y.a in Southern California, and its growing extension reached the Bay Area from Southern California 12 m.y.a. (Stoffer 2006). Between 8 m.y.a. and 3 m.y.a., the Pilarcitos Fault zone was responsible for 120 km of the northwest offset of the sheared-off portion of the North American plate (which includes Point Reyes), while the San Andreas Fault zone became accountable for the NW slip 3 m.y.a, with a total offset so far of 35 km. The active San Gregorio fault zone to the southwest (not shown and mostly offshore) accounts for a total of about 155 km of the NW lateral movement of the North American

plate starting 8 m.y.a. (Brabb, Graymer, & Jones 1998). Additionally, an estimated 174 km of the NW offset is accounted for by faults in the San Francisco East Bay fault zone starting 12 m.y.a., when the San Andreas system first arrived in the Bay Area (Stoffer 2006).

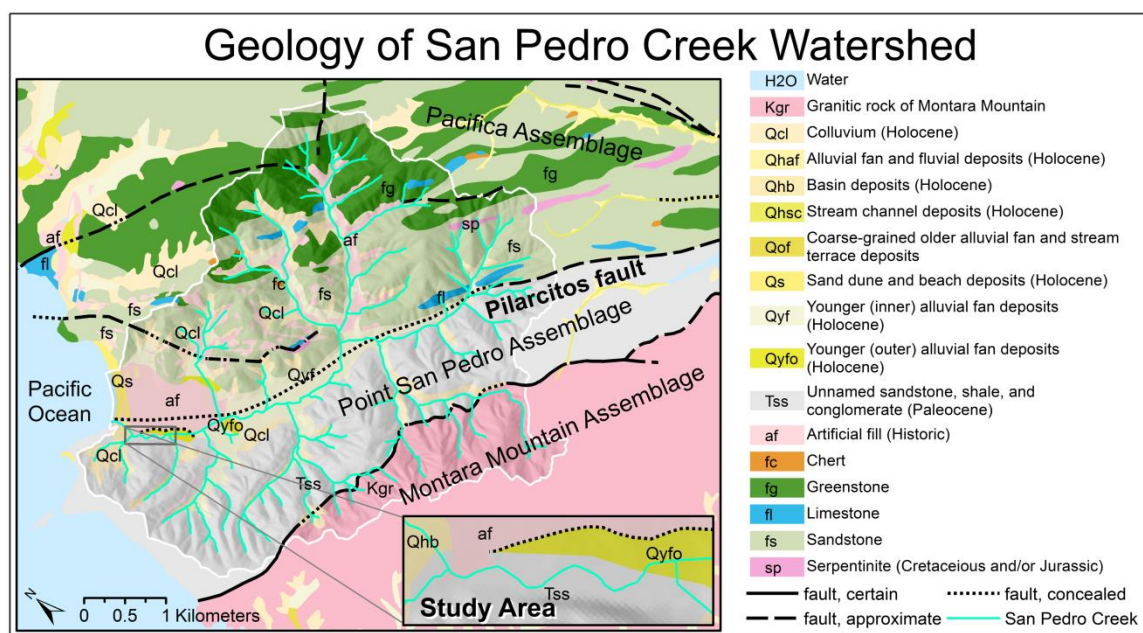


Figure 6: Geology of San Pedro Creek watershed. Modified from Brabb, Graymer, & Jones (1998). Please see original for the details of geological units.

North of the stream reach is the Pacifica Assemblage, demarcated by the Pilarcitos fault just north of the creek mainstem, which veers SSE outside of Pacifica, and the San Andreas fault to the northeast (Figure 5 and Figure 6). The Pacifica Assemblage includes material from the Cretaceous and Jurassic consisting of greenstone and sandstone, which is interspersed with bands of limestone, serpentine, and chert. To the south of the Pacifica Assemblage is the Point San Pedro Assemblage demarcated to the north by the Pilarcitos Fault and to the south by an unnamed fault along the Montara Mountain Assemblage. The southern tributaries of San Pedro Creek extend into the granites of the Montara Mountain Assemblage and flow down into the Paleocene sandstone, shale, and conglomerate of the Point San Pedro Assemblage. The mainstem runs roughly SE to NW

and straddles the boundary between the Point San Pedro Assemblage and the Pacifica Assemblage, with streambanks incising into Holocene colluvium.

Within the stream reach alluvial materials dominate, with outcrops of erosion resistant materials that could be either bedrock from the Point San Pedro Assemblage of sandstone, shale, and conglomerate or Quaternary clays. Sediment supply includes gravels and fines from the Middle Fork and limestone, shale, and granitic cobbles from the South Fork (Davis et al. 2004).

### **San Pedro Creek as habitat**

Central California steelhead (*Oncorhynchus mykiss*) do not die after spawning and may leave and return to spawn in their natal stream two to three times in their lifetime (Johnson 2005). In 2003 and 2004, there were a significant number of two-year old steelhead in the upper reaches of the mainstem, but the lower reach lacked significant numbers of any age group (Johnson 2005). However, the 500 m lowermost reach of the mainstem (the study area) is at least an important fish migration corridor, and Johnson (2005) found that in 2004 the post-restoration reach had potential to provide habitat for spawning and/or fingerlings by way of an increase in undercut banks and overhanging vegetation. The study area is also suitable habitat for the federally-listed endangered California red-legged frog (*Rana aurora draytonii*). At least one individual was identified prior to the restoration (Lee 1999) and another individual was identified during the reach restoration and documented in USACE photography (Figure 7). The California red-legged frog was relocated during electrofishing and fish relocation (Figure 8) in 2002, which was implemented before routing stream flow to the new channel. A third special status species that may occur in this habitat is the San Francisco garter snake (*Thamnophis sirtalis tetrataenia*), which prefers California red-legged frogs as its food source.



Figure 7: California red-legged frog on SPC measured during fish relocation before re-routing the stream discharge into the new channel in 2002. Photo courtesy of USACE (2013).

Unfortunately, salmonid habitat can be degraded by sedimentation in the stream, including from the fines from landslides and gullyng in the upper reaches (Davis et al. 2004), which may bury spawning gravels and affect salmonid food sources of aquatic invertebrates (Collins 2001). Bedloads of greater than 30% fine sediments ( $< 6.35$  mm) are associated with  $< 50\%$  survival of salmonid fry from spawning nests to emergence (Kondolf 2000, Pearce et al. 2004). Collins, Amato, and Morton (2001) found the D50 sediment class size on the SPC FCP reach to be fine gravels at 18% (4–8 mm), along with less than 4% silt and clay, 24% sand ( $< 2$  mm), 11% very fine gravel (2–4 mm), and 42% medium, coarse, or very coarse gravel (8–64 mm). These numbers indicate an excess of fines (39% of sediments were  $< 4$  mm) and a deficiency of coarse gravels, and consequently unsuitable habitat for steelhead spawning.



Figure 8: Steelhead fingerling on SPC relocated during the discharge re-routing to the new channel in 2002. Photo courtesy of USACE (2013).

Additionally, water quality monitoring demonstrates fecal contamination that may come from both anthropogenic and resident wildlife sources (Ivanetich et al. 2006). Sassoubre et al. (2011) modeled fecal indicator bacteria on SPC using water samples and concluded that zero order reaches above the urbanized North Fork were the most likely sources. Additionally, the FCP study area wetland did not have a filtering effect for the fecal indicator bacteria, being detected equally both up and downstream of the reach.

Despite years of maintenance as a straightened channel, the pre-restoration stream reach corridor had developed riparian vegetation (Collins, Amato, & Morton 2001) and stream habitat suitable for steelhead and California red-legged frogs. In an effort to enhance this habitat, the City of Pacifica (CP) worked with USACE to acquire the adjacent dirt lot, design a natural meander and floodplain, and revegetate with willows, alders and other native plants. This ecological restoration was part of the flood control effort.

## RESTORATION AND FLOOD CONTROL

### **SPC channel design theoretical values**

For the San Pedro Creek Flood Control Project (SPC FCP), geomorphological restoration planning is more a re-imagining of a more natural stream than the reestablishment of an actual preexisting condition. For one, detailed pre-1900 watershed variables are largely unknown, such as the extent of sausals or Lake Mathilda in the valley, or the form and discharge of stream channels. Furthermore, even if those details were available, the site has changed and they would be logistically difficult to recreate given the urbanization and associated changes in discharge, sediment supply, and valley functions (Lee 1999).

Along with the physical changes, like increased impervious surfaces and continuous pumping of historic lagoons, the processes of a watershed will change. For example, urbanized areas can contribute to flashier instream storm responses and to new sediment sources from gullies or stream capture (Kondolf 1998, Wilcock 2012). Additionally, local land management practices may shift, for example, to include removal of woody debris from streams, to stop controlled burning maintaining grasslands, or to eliminate grazing.

Degraded streams in urbanized watersheds that are designated for restoration need both an assessment of anthropogenic influences on stream processes as well as a natural stream assessment. When organizing a stream restoration design, similar nearby watersheds or stream reaches provide potentially useful models of form and process. These are called reference reaches. Additionally, estimates of appropriate bedform and floodplain geometries, among other variables, are regionally available based on local precipitation and watershed size. These are called regional curves. When historical data for a particular site are not available, both reference reaches and regional curves can help approximate local conditions.

Dunne and Leopold (1978) created the original San Francisco Bay Area regional curves predicting bankfull channel dimensions from watershed drainage areas, assuming approximately 760 mm annual precipitation (Figure 9). San Pedro Creek Watershed has 956 mm average annual precipitation, 25% greater than the precipitation factored into Dunne and Leopold’s (1978) curves. Nevertheless, the regional curves are included here for lack of San Mateo County or coast-specific curves, and for comparison to other San Francisco Bay Area curves. Using estimated equations for their graphs, which did not originally include equations, the curves predict the SPC watershed of 21 km<sup>2</sup> to have a bankfull cross-sectional area of 7.8 m<sup>2</sup>, bankfull width of 9.4 m, and bankfull depth of 0.8 m. Dunne and Leopold (1978) did include the equation to estimate bankfull discharge in the Bay Area, where for a drainage area of (x) in km<sup>2</sup>, there is an associated discharge (y) in m<sup>3</sup>/s. They again also assume approximately 760 mm annual precipitation. Their equation is given as  $y = 0.6194x^{0.93}$ . With a drainage area of 21 km<sup>2</sup>, the calculated bankfull discharge for San Pedro Creek would be 10.5 m<sup>3</sup>/s.

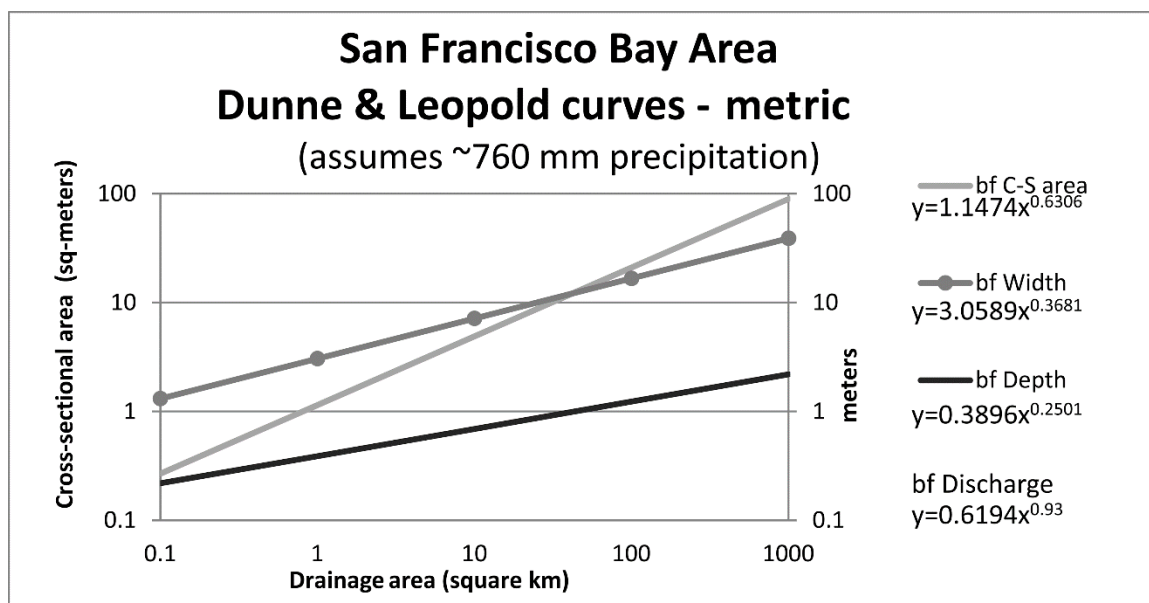


Figure 9: Bankfull dimensions by drainage area based on equation approximations of the regional curves presented in graphs from Dunne & Leopold (1978). The bankfull discharge equation for the SF Bay area was included in their text and is included in the legend above.

Davis (2008) compared the SPC FCP theoretical morphological variables to the as-built FCP planview meander shown in 2004 aerial imagery. His calculated values are based on a drainage area of 19 km<sup>2</sup> and input into Dunne and Leopold (1978) regional curves as modified by Ann Riley (2002) for the San Francisco East Bay. Theoretical results included bankfull width (9 m), meander wavelength (100.8 m), radius of curvature (20.7 m), and pool spacing (45–63 m). On the other hand, his measured wavelength for four of the meander bends in the as-built restoration reach averaged 154 m (54% longer). His backwards calculation using the Ann Riley (2002) regional curves then predicts an associated bankfull width of 14 m and pool spacing of 70–100 m.

The Dunne and Leopold (1978) Bay Area regional curves were modified and expanded for Marin and Sonoma County in the North Bay by Collins and Leventhal (2013), while the San Mateo County (the study area county) updated local curves are due in 2016 (San Francisco Estuary Partnership 2014). The Collins and Leventhal (2013) curves do not presuppose a specific annual precipitation and are interpolated from stream channel field observations in the North Bay counties of Marin and Sonoma, but not San Mateo, where SPC is located. Nevertheless, using the curves for comparison, we get bankfull variable estimates for the SPC 21 km<sup>2</sup> drainage area, including bankfull area (7.1 m<sup>2</sup>), bankfull width (10.4 m), and bankfull depth (0.7 m). Other design variables predicted by the curves are: 12.3 m<sup>3</sup>/s bankfull discharge with 1.7 m/s bankfull mean velocity, 24.7 m floodprone width for a stable channel, and a bankfull depth to mean depth ratio of 1.44. It is noteworthy that the Dunne and Leopold (1978) bankfull width for SPC (9.4 m) is between the modified East Bay curves value (9 m) (Davis 2008) and the North Bay curves value (10.4 m) (Collins and Leventhal 2013). See Table 1 for a comparison of SPC FCP stream reach variables from the literature and planning documents. Finally, Collins and Leventhal (2013) estimate a mean Manning's n value for a Rosgen C4 stream reach to be 0.037 (between approximately 0.028 and 0.044).

Year:	1978	1995	2008	2008	2013	2013
Source:	Dunne & Leopold	Lee (forms)	Davis (theory)	Davis (as-built)	Collins & Leventhal	HEC-RAS / USACE
Bankfull width (m)	9.4	15.24	9	14 (given $\lambda$ )	10.4	47 (2-year @CS2)
Bankfull depth (m)	0.8	0.76 (av)			0.7	
Bankfull area (m <sup>2</sup> )	7.8				7.1	
Discharge (m <sup>3</sup> /s)	10.5	12.74			12.3	19.8 (2-year)
Wavelength, $\lambda$ (m)		137.2	100.8	154		
Radius of curvature (m)		38.1	20.7			
Pool spacing (m)			45–63	70–100 (given $\lambda$ )		
Manning's n		0.02 (0.03/0.1 fp*)			0.037 (.028–.044)**	0.042/0.15 fp

\* Value from USACE (2013) labeled "design Manning's n"  
\*\* For a C4 Rosgen stream type

Table 1: SPC FCP restoration theoretical values from the literature and planning documents.

Knighton (1977) describes meander variable value ranges taken from the literature given a stream discharge and its associated channel bankfull width. The radius of curvature is generally 2–4 times bankfull width. Meander wavelength is approximately 7–10 bankfull widths, with riffles in the straight reaches between the meander bends. A meander, by his definition, has sinuosity of greater than or equal to 1.5. Williams (1986) found a pattern of 1–7 bankfull widths for radius of curvature, averaging 2.4 as compared to an earlier study by Leopold and Wolman (1960), which had included sinuosities <1.20 and found a wider range of 0.84–9.7. Additionally, the longest straight reach ought to be 10 times the bankfull width, the radius of curvature ought to be to 2–3 times bankfull width, and the meander width ought to be 4–5 times the radius of curvature (Knighton 1977). Keller (1972) further locates pools on bends and riffles at inflection points. This echoes Leopold, Wolman, and Miller's (1964) ideal formation of two pool riffle sequences per meander wavelength, each approximately 5–7 bankfull widths long.

On SPC, Davis (2008) found a theoretical pool spacing for FCP of 45–63 m based on Riley (2002), but a back calculation based on the as-built FCP meander wavelength (154 m) found that wavelength would theoretically have a designed pool spacing of 70–100m. Lee's (1995) design documents specify a meander wavelength of 137.3 m, but do not include pool-riffle spacing. Using the Lee (1995) design bankfull width of 15.24 m and the above relationships, we get theoretical values for pool-riffle spacing (76–107 m), meander wavelength (107–152 m), and radius of curvature (30–46 m). The pool spacing

is similar to the as-built Davis (2008) backwards calculations, where the meander wavelength is lower than the as-built. The as-built radius of curvature measured from Davis (2008) is 33 m and is consistent with the theoretical value given the Lee (1995) design bankfull width.

The San Pedro Creek FCP restoration designers, Lee (1995, 1999), explored 56 potential reference sites along the coastline from Pacifica southward to Santa Cruz in the search for appropriate comparative restoration bedform and planform variable values. The stream design is based on Hydrogeomorphic (HGM) wetland classification, which focusses on ecosystem functions by creating indices to compare reference sites with degraded, restored, and constructed landscapes (Lee 1999). After analysis, only 3 of the reference streams were found to fit the study area HGM characteristics adequately, noted as both a Rosgen C4-5 classification stream (Lee 1995) or a Rosgen B4-5 type (Lee 1999). The change from type C to B during the design process may have been to account for lower designed sinuosity. The reference sites had a D50 sediment size of sand (.0062–2 mm), where the FCP pre-restoration D50 was found by Lee (1999) to be gravel (2–64 mm), which is consistent with Collins et al. (2001) for the FCP pre-restoration D50.

Lee (1995) also presents the Rosgen (1994) bedform design variables for the SPC restoration project, including a radius of curvature (38.1 m), meander wavelength (137.2 m), W/D ratio (20), sinuosity (1.33), bankfull width (15.2 m), mean depth (0.76 m), and maximum depth (1.22 m). However, Lee (1999) design documents show the stream variables change slightly, including for bankfull width (17.7 m), meander wavelength (152.4 m), W/D ratio (29), and sinuosity (1.3). The Lee (1995) 1-year flood return discharge is noted as 12.7 m<sup>3</sup>/s, while the 2-year is between 19.3 to 19.8 m<sup>3</sup>/s. The 15.2 m value is repeated by USACE and CP (1998) as the width for the FCP “lowflow channel” (p. 26), which would have a capacity of 99.1 m<sup>3</sup>/s discharge and meander across a floodplain/wetland of width 64 m. The Lee (1999) design intends to create a bankfull

return interval of 1.0–1.3 years to encourage overbank flow into the wetland/floodplain at least annually and to maintain pits (14% of floodplain), sloughs (14%), secondary channels (21%), and off-channel ponds (7%). To do this, the designers attempted to generate the longest possible stream channel within the floodplain.

To estimate bankfull return intervals, geomorphologists would prefer to look to site-specific indicators of bankfull, such as erosion and deposition, riparian vegetation patterns, and wetted surface, and then use permanent long term stream gauge data to calculate bankfull return intervals. When these data are not available, regional curves and reference sites with data must suffice. The fieldwork of Collins and Leventhal (2013) in Marin and Sonoma Counties confirms the fact that urbanized streams have more frequent peak flows due to higher drainage densities (for example, from culverts and storm drains) and faster urban run-off. They calculate that the bankfull, or effective, stream discharge return interval in Bay Area urban areas is not 1.3–1.7 years, but instead more frequent, in the range of 1.1–1.3 years. Using this, the Collins and Leventhal (2013) bankfull estimate for SPC FCP would be a 12.3 m<sup>3</sup>/s discharge for a 1.1–1.3-year return interval. This is nearly equal to the USACE (1998) value of 12.74 for a 1-year return discharge and the Lee (1999) value for bankfull, with return of 1.0–1.3 year return. It will be interesting to see in 2016 if these return interval discharge values are maintained when the San Mateo County/SF Peninsula regional curves are presented.

### **Flood capacity modeling and USACE design variables**

USACE uses the Hydrologic Engineering Centers River Analysis System (HEC-RAS) to model floods using inputs such as cross-section area, discharge, and Manning's n. It is a one-dimensional model because it does not include 2D and 3D data such as bedform or planform shape into the model calculations. Received in 2012 as part of a 2011 Freedom of Information Act (FOIA) request made to USACE, their preliminary HEC-RAS flood model for the SPC FCP restoration reach was found to utilize cross-sectional data from a

contractor, Towill, who acquired the data of FCP in 2011, along with USACE custom regional curves for discharge and custom values for Manning's n/roughness.

The 2011 contractor cross-sectional data, and other variables, were inputs into the HEC-RAS model and help visualize the flood scenarios of different flood return intervals. The 2-year return interval discharge value is given as 19.8 m<sup>3</sup>/s and the 100-year flood return level discharge is 100 m<sup>3</sup>/s (USACE 2013). The lowest return interval is 2 years and there are no values labelled as bankfull. Using the 2-year return interval as a proxy for bankfull, the USACE bankfull discharge value is 61–89% higher than the calculated values above of 10.5 m<sup>3</sup>/s and 12.3 m<sup>3</sup>/s. The USACE and CP (1998) 1-year return interval flood discharge of 12.75 m<sup>3</sup>/s is not included in the HEC-RAS Peak Discharge vs. Frequency Curve or flood model. The 1-year value, as well as their 2-year and 100-year values, are based on Branciforte Creek in Santa Cruz County, which is a gauged stream of a similar sized watershed (USACE and CP 1998). Lee (1999) uses this 1-year value for bankfull in the Rosgen stream design form included in the report. A selection of USACE's HEC-RAS input variables are graphed below in Figure 10, Figure 11, and Figure 12. Seasonal roughness, sediment supply details, and unsteady flow data, among other inputs, are absent from the model and are not required for the model to run.

There were four total variations of the HEC-RAS flood model included in the responsive documents from the USACE FOIA request. The four variations are bridge as-is with design Manning's n, new bridge with design Manning's n, bridge as-is with proposed Manning's n, and new bridge with proposed Manning's n. The first bridge variation is the Highway 1 Bridge as it was, with a 4.35 m clearance elevation and a thalweg elevation under the bridge of 2.26 m. The second is the bridge as-proposed for the Highway 1 Bridge restoration, which started in 2014. This as-proposed bridge is represented with a clearance elevation raised 1.5 m to 5.85 m. The new bridge also has an approximately 18 m wider stream clearance.

Then for each of the two bridge variations, the model runs two different sets of Manning's n values. The first is noted as from the "design" and uses Manning's n values 0.03 (instream) and 0.1 (floodplain). However, Lee (1999) design documents show a Manning's n value estimated at 0.02. The second set is labelled as "proposed" and could be USACE's own proposed Manning's n values. This set has values of 0.042 (instream) and 0.15 (floodplain). Both the design and proposed values are within the range of Collins and Leventhal (2013) Manning's n values (0.028–0.044) for C4 Rosgen stream reaches for streams in the North Bay. However, the Lee (1999) value is lower and is not differentiated between instream and floodplain, stated as due to the narrowness of the floodplain not affecting roughness like the reference reaches. The higher proposed Manning's n values used by USACE may account for the increase in vegetation since the design and installation of the reach before the revegetation.

In Figure 10, increasing stream discharge rates correlates with rises in the water surface elevation. The upstream end of the SPC FCP reach is labeled Upstream and the lower end of the reach is Hwy 1. They are displayed together to show the upper and lower bounds of water surface elevation in the flood control project reach of San Pedro Creek. Note that the labelled points are the 2-year flood return interval levels, with equivalent  $19.8 \text{ m}^3/\text{s}$  discharge values. These points mark a visible change in the rate of rise of the water surface elevation where the steeper rise has discharges under  $19.8 \text{ m}^3/\text{s}$ . This set of data points taken from the HEC-RAS models corresponds with geomorphological theory that below bankfull discharge the water level changes more quickly relative to discharge than above. This is because the geometry of the incised channel has steeper banks as compared to the wider floodplain.

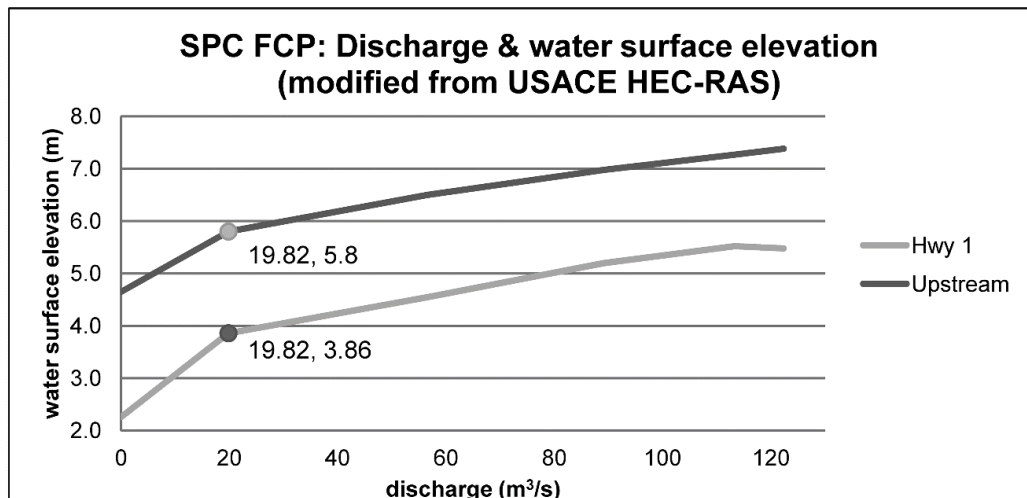


Figure 10: Discharge and water surface elevation downstream and upstream of the study area. Elevations based on the vertical datum NAVD88. Note that 19.82 m<sup>3</sup>/s is the 2-year flood return interval discharge value.

The width variable in Figure 11 has no values above the 50-year return interval because the HEC-RAS model cannot model beyond the cross-sectional extents, which were reached at 50-years in this cross-section just upstream of Highway 1. Figure 12's width variable does not end at the 50-year flood return interval, but instead shows a complete set of increasing widths up to the 500-year flood return interval. It was included here as one of the only HEC-RAS USACE cross-sections where the width variable did not reach the (narrow) model extent for even a 500-year flood.

The trendline for a USACE HEC-RAS flood return interval curve formula is:

$y = 18.569\ln(x) + 11.708$  with  $x$  being years and  $y$  being discharge values. It is derived from Figure 11 and Figure 12. Using the trendline equation, a 2-year flood return event would produce a 24.6 m<sup>3</sup>/s discharge in the study area, higher than the actual value used in the HEC-RAS model, 19.8 m<sup>3</sup>/s. A 1-year flood return interval event would produce a 11.71 m<sup>3</sup>/s peak discharge, which is just under the USACE and CP (1998) estimate of 12.75 m<sup>3</sup>/s.

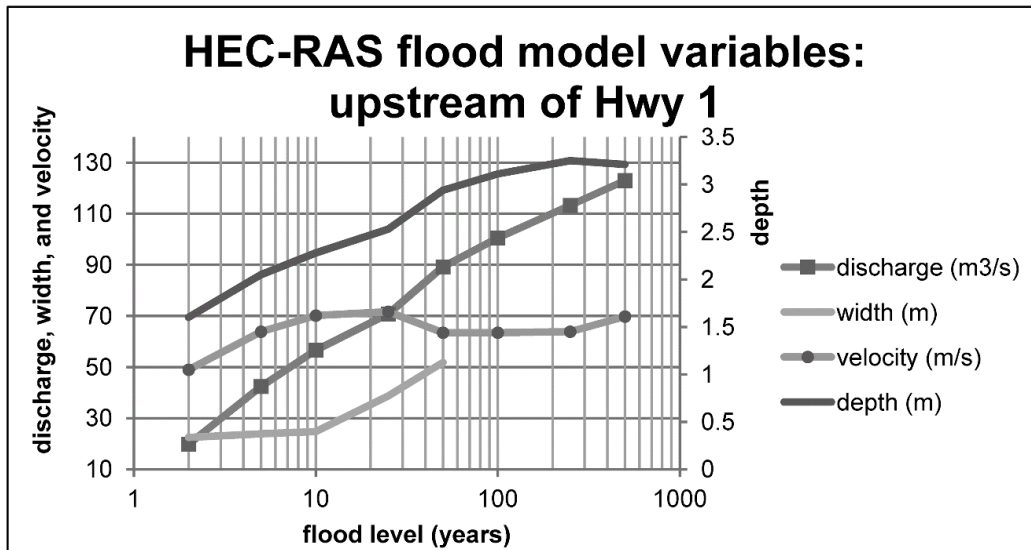


Figure 11: Model variables upstream of Highway 1. Notes: Model discharge (Q) is the same at each cross-section for one flood return interval value. An approximate equation for Q is  $y = 18.569 \cdot \ln(x) + 11.708$ . However this does exaggerate the 2-year return interval flood value of 19.8 to 24.6 m³/s.

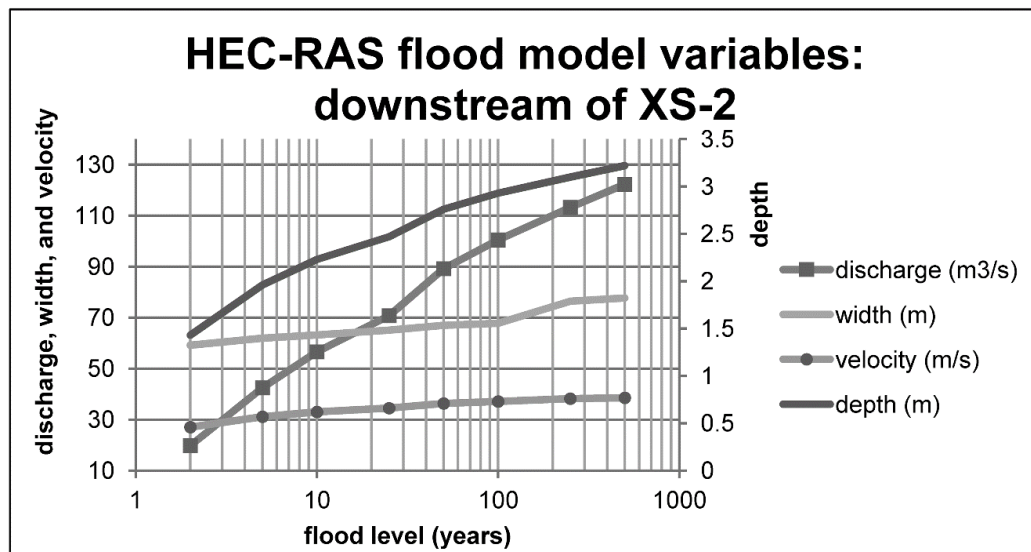


Figure 12: Model variables near cross-section 2 (CS2/X-S2), discussed later in this paper, taken from USACE's HEC-RAS flood model.

**Daily precipitation data, discharge, and return intervals**

San Pedro Creek does not have a stream gauge but there are daily rainfall data available.

It would be useful if rainfall data return intervals could be used in lieu of stream gauge

data to estimate the level of flooding. Return intervals for storms and floods are based on the annual maximum daily precipitation and the annual peak daily discharge, respectively. The list of annual maximum daily values for all years are sorted and ranked (rank 1 is the greatest) and then used to calculate return intervals. The highest return interval possible with a set of data is equal to the number of years of data plus one.

In rain-dominated watersheds with aridity indices (AI) close to one, the annual peak daily discharge event is likely to occur within a 5-day window after the annual maximum daily precipitation event (Guo et al. 2014). Weiss et al. (2013) maps Pacifica, California with an approximate average precipitation (P) of 950 mm and an approximate average potential evapotranspiration (PET) of 1100 mm. With  $AI = PET/P$ , the SPC Watershed has an AI of 1.16, showing that this 5-day window links a particular year's maximum precipitation and discharge. However, large flood events, with long return intervals, can occur in response to only average annual maximum daily precipitation events, with much shorter return intervals. Therefore, a precipitation event with a known return interval does not predict the level of flooding (Guo et al. 2014).

The correlation of the two return intervals, unfortunately, can depend on water balance variables in the watershed such as antecedent moisture content, event runoff coefficient, and basal flow index (Viglione, Merz, & Blöschl 2009, Guo et al. 2014). A 1.5-year return interval storm initiated when the ground is relatively dry will create a lower discharge and flood return interval event than the same precipitation event initiated after the ground has already been saturated. In simulation models, the flood return interval is always less than the precipitation return interval (Viglione et al. 2009). However Viglione et al. (2009) did find that wetter areas, like SPC, have higher and more frequent flood peaks, but with low flood return intervals. This contrasts with dry areas that may have less frequent flood peaks, but they will have higher return intervals. In order to predict the relationship between storm return interval and flood return interval, variables such as

event runoff coefficient, storm duration, and the threshold of runoff generation can be helpful (Viglione et al. 2009). On SPC, we do not have storm duration times or an estimate of the threshold of runoff generation. Nevertheless, using daily rainfall data to calculate the annual maximum daily precipitation per year and the associated storm return interval curve for SPC yields a limited understanding of the local precipitation and discharge relationships during particular storms and flood events on the reach.

### **SPC restoration installation**

The restoration of SPC took place between 2001 and 2004. Eight feet of urban fill was removed, the exposed soil was ripped and turned with new added soil, and the floodplain extent was regraded. Then, because the reference sites with stream access to floodplains had temporary and permanent water storage morphology outside of the main channel (pits, sloughs, secondary channels, ponds), the Lee (1999) design attempted to duplicate this floodplain complexity and connectivity with hummocked topography. This was followed by the initial channel dig in 2002.

Lee (1995, 1999) designed the meander and floodplain geometry along with the revegetation scheme. The restoration project included vegetation plantings of willows and alders on the banks and floodplain, along with approximately two dozen native plants from 11 different community groupings (TRA Environmental Sciences 2007). In 2007, 90% of the Section 205 area had greater than 80% native species, presumably residuals of the mass plantings from 2001–2003 (TRA Environmental Sciences 2007).

After the revegetation with seedlings throughout the floodplain, the area was irrigated for approximately one year until 2003. In 2004, vertical logs (also known as rootwads) were installed to stabilize footer log revetments along meander bends in the new channel. Before diverting the flow to the new channel, the meander bends were modified at the north side, cutting up to the pre-restoration channel, which was then filled.

Overall funding for the project was just under \$11 million, with \$7 million coming from USACE and approximately \$4 million coming from local contributions (USACE 2014). This does not include the approximate value of the land acquired from the California Department of Transportation (CalTrans) in 1998 (McDonald 2004). In the exchange, CalTrans wanted wetland mitigation credits for a new bypass tunnel just south of the watershed (McDonald 2004). USACE valued the property at \$6,656,000 (“real estate lands & damages”) in 1997 prices (USACE 1998). USACE also allowed for further request for funds, potentially for the Highway 1 Bridge widening of 2014 and 2015, which is under the jurisdiction of CalTrans (USACE 2014).

In their planning documents, USACE states that the City of Pacifica is pleased that the project will provide 100-year flood protection while enhancing natural habitat. However, USACE also defines the 100-year flood protection as mitigating flood damages, not altogether preventing them. In particular, they state that a mean 100-year flood will cost only \$75,000, versus \$2.352 million without the project. USACE maintains that the banks in the wetland restoration should remain stable indefinitely and that operation and maintenance (at a cost of \$8,570 annually) will enable local managers to prevent revetment blowouts or bank failures (USACE 1998).

Two significant changes were made after the finalized Environmental Impact Statements (EIS) reviewing the 75% design in USACE and CP (1998). First, a culvert bypass channel was eliminated. The bypass would have taken overflow from an upstream bridge into the study area, via an underground pipe to be installed beneath roads and residential lots, and joining an existing culvert, which drains into the study area from the southeast (USACE and CP 1998, McDonald 2004). It was abandoned due to cost and local disinterest (McDonald 2004) and instead the existing culvert continues to connect only three storm drains to the restoration floodplain area (USACE 1998), including from

Bower Road and San Pedro Terrace Road, both to the south of the reach. USACE (1998) states that there are “no significant tributaries” (p. 11) within the FCP reach and that the flows from the existing culverts will be routed through the FCP wetland to reduce flow velocity. The No-Action Alternative for the bypass culvert in the EIS was used and states that any impact to utilities affected by flooding would not be significant (USACE and CP 1998). However, there is a natural subwatershed uphill from this culvert that is 0.4 km<sup>2</sup>.

Second, the as-built meander planform channel is different from the Lee (1999) design. During the fill removal and re-grading, the contractors unearthed an Ohlone shellmound carbon dated to be from 1010 to 1410 AD, despite previous, repeated, and extensive archeological surveys of the restoration area finding absence of an archeological site (Lee 1999, Ungvarsky 2002). The shellmound was also not mentioned in subsequent monitoring reports in 2001, 2003, 2004, 2006, or 2007. In the end, no USACE or contractor documents mention the shellmound or the last-minute meander redesign to circumnavigate it, while the Ungvarsky (2002) report remains a draft report. At the least, Ungvarsky (2002) documents correspondence from contractor to the most likely descendants, the Muwekma Ohlone Tribe, who did not voice any specific requests for the site beyond what the contractor proposed: returning unearthed fragments, mesh covering and dirt overfill, and re-worked design to avoid shellmound disturbance. However, no as-built planform design exists in any of the FOIA requested documents.

Two additional deviations from the original approved plan are the deferral of the widening of the Highway 1 Bridge and the permanent decommissioning of the local road paralleling the stream reach to the south, San Pedro Terrace Road. Lee (1999) mentions that safety concerns regarding the local road impacted the floodplain design. In 2014, the bridge reconstruction was underway while San Pedro Terrace Road was being used recreationally for cyclists and pedestrians.

### **Meander and channel adjustment theory**

Given the need for channel stability in urban streams, understanding the long term system adjustments due to natural geomorphic processes is central to assuring the ongoing success of the joint efforts of ecological restoration and urban flood control. In an urban stream restoration such as SPC FCP, selecting the design meander wavelength involved estimation of design variables for a degraded stream system. If the installed channel were too small to accommodate the local stream discharge and sediment supply, channel banks would be expected to overtop frequently. Wilcock (2012) criticizes the practice of encouraging overbank flow, but Lee (1995) states that wide meanders will increase floodplain roughness needed to dissipate energy with flow along banks and point bars acting “as brakes” on the flow (p. 40). This overbank flow will also encourage particle retention and wetland complexity. On the other hand, if the installed meander wavelength was too large, then the adjustment processes of erosion and deposition might eventually produce shorter meander wavelengths with associated shorter meander amplitudes.

Designing regular overbank flows was shown in a flume experiment to encourage the deposition of material into the floodplain and grow it, while also growing point bars to the level of the floodplain and filling in possible chutes with fines (Braudrick et al. 2009). After an initial rapid meander migration, the model demonstrated a steady 0.5 to 0.7 channel widths migration rate per year equivalent. The inclusion of fine materials ensured meander morphology by limiting the bank erosion to the rate at which bars could grow. Without the fines, the bars did not grow to the elevation of the floodplain, which resulted in large chute cut-offs. Vegetation (alfalfa sprouts in the flume model) could delay the chute cut-offs but fine sediments were required to prevent island bars. Braudrick et al. (2009) conclude that sands should not be limited in gravel bed systems.

Luchi, Zolezzi, and Tubino (2010) illustrate two types of two-phase sinuosity meanders. The first type is an underfit stream, which has too low of discharge for the channel

dimensions. New incisions and meanders form within the wider previously incised stream channel, thereby creating a shorter wavelength meander wandering within the longer-wavelength and wider channel. Their second type of two-phase sinuosity occurs when the active channel width is the same as a shorter wavelength channel width, but like a fractal, the finer scale view has a meander form as well. This second type may be wider at the bends of the longer wavelength phase, with point bars like a typical meander, or have no change in width at the longer wavelength meander bends. Either way, an increase in curvature of the smaller wavelength within the larger meander wavelength creates a bimodal sinuosity that presents itself as a meander pattern within a meander pattern. In SPC, the design was a larger meander, and the adjustment to a smaller meander might appear like the second two-phase type described. Additionally, SPC would be expected to have an excess of point bars and pool-riffle sequences within one meander wavelength.

Two mechanisms for central bar formation in meandering streams are modeled by Luchi et al. (2010). The first mechanism occurs in a channel with longitudinally varying channel widths. A symmetric diversion of water flow to both banks in wider cross-sections forces a central bar to emerge. The second mechanism involves the secondary flows associated with meander planform, which are known to produce point bars in linear models. With Luchi et al.'s (2010) non-linear model, mid-channel bars formed in channels with too large of meander wavelengths, such as in SPC, and concentrated just downstream or upstream of meander bends by a few channel widths. These mid channel bars widened the stream. In the model, this process was followed by a scour pool near the inflection point, downstream of the meander, where the split thalweg rejoins itself, and also where narrowing results. Applying this model to SPC FCP, where there are no channel width variations in the meander design, would place it within the second mechanism of both point bar and channel bar formation. However, channel width variation was found by Luchi et al. (2010) to develop after mid-channel bars formed with the secondary flow. Similarly on SPC, once mid-channel bars form and there are width

variation, then there is the potential for the interaction of both mechanisms described in the model.

Gay et al. (1998) describe chute cut-offs on Powder River in Montana, observed over many decades, which were initiated downstream of meander bends at the point of inflection, rather than upstream from bank overtopping and direct incision of a new channel. This chute cut-off is a meander adjustment in confined valleys, as opposed to neck cut-offs, which occur in unconfined valleys (Rutherford 1994, Hooke 2003). A case study using historical maps of an English river supports the theory that meander growth and cut-offs oscillate around an equilibrium sinuosity, where low flows increase the meander bend and peak flows create cut-offs (Hooke 2003). In a particular cut-off, Hooke (2003) theorizes that a steep riffle headcut up the bank led to a chute cut-off. Similarly, Gat et al. (1998) observed that water upstream overbanks during floods and flows linearly downslope (instead of meandering through the channel) and the inflection points serve as a point of re-entry to the channel. Like an underwater cascade, the erodible bank begins to headcut. Subsequent floods were found to either extend the headcut erosion, complete the headcut into a chute cut-off, or abandon the new partial channel. SPC is a much smaller stream, but has erodible banks at inflection points and has frequent overbank flow by design to allow the floodplain and wetland development. Therefore SPC could experience this type of headcut erosion and chute cut-off at inflection points.

Jurmu (2002) found that stream variables and processes for unmodified (non-coastal) wetland streams in three case studies in different U.S. states can vary from those in alluvial streams. In the case of SPC, the floodplain is valley alluvium and does not appear to have salt water intrusion into the FCP reach, despite the area historically supporting the tidally influenced fresh water to brackish lagoon Lake Mathilda (Lee 1999). Nevertheless, with sea level rise the FCP reach could become a tidally influenced coastal

wetland like the area just downstream of Highway 1. In this case the function and design controls in the reach may not function like they would in a typical alluvial stream. Jurmu (2002) found that meander bend spacing was erratic in upland wetlands, bend cross-sections lacked point-bar and cut bank asymmetry, and that relationships between channel width, radius of curvature, and axial length were atypical when compared to alluvial streams. Additionally, two of the three wetland streams had riffle widths less than pool widths, which is atypical of alluvial streams. Along with the urban stream dynamics and the limited floodplain extent complicating the analysis of this reach, climate change and sea level rise could contribute further variability.

## METHODS

### **Fieldwork**

The primary goal of the 2007 and 2011 fieldwork was the acquisition of longitudinal profile and three cross-sections data points using a digital level. Data were also available from previous surveys of the stream reach from 2003, 2004, and 2005.

The longitudinal data are compared for 2003, 2005, 2007, and 2011 and assessed for patterns of aggradation and degradation. There were also fieldwork data for three cross-sections. Cross-section 1 (CS1) includes three survey years: 2004, 2007, and 2011. Cross-section 2 (CS2) includes 2007 and 2011. These two cross-sections both have supplemental survey data for 2004 floodprone area and for USACE's 2011 cross-sections and floodplain extents for bankfull and 100-year flood. Cross-section 3 (CS3) includes 2007 and 2011 data, but has no supplemental data from earlier years or USACE. Pebble counts at the three cross-sections were done for years 2007 and 2011.

There were significant errors in the compass direction, or horizontal circle (HC), for field points acquired using the digital level in 2007 and 2011. This was due to either human error in manual recording or possibly magnetic interference. The HC was a required input for the trigonometric formulae used to convert the data into either longitudinal profile points (distance along thalweg with thalweg elevation) or into geographic coordinates. Control points in 2007 and 2011 collected with a GPS receiver with an average of 10 cm accuracy provided guidance in correcting the point errors.

Adjustments to correct errors propagated by the HC errors involved translation of point groups to line up with control points, rotation of point groups to maintain *distance* between points (assumed to be correctly recorded by the data logger), and the maintenance of *angles* between point clusters acquired from the same data collection set-

up location (assumed to have the same initial HC error). Supplemental guidance came from a raster digital terrain model (DTM) created from the 2011 LiDAR, high-resolution streambed breaklines, aerial orthophotography, and field notes and sketches.

LiDAR elevation data used the vertical datum NAVD88. However, the LiDAR field survey did not include the nearby US Coast Geodetic Survey marker or any of the same points as the fieldwork for this study. The survey marker Y1240 was established on the Highway 1 Bridge in 1972 as a benchmark. To compare LiDAR and fieldwork data, all fieldwork elevations were adjusted by adding 0.64626 m in order to match the NAVD88 elevation of the Highway 1 benchmark.

### **Remote sensing and planview measurements**

Planviews of the stream reach over time were hand digitized from USGS orthoimagery from before, during, and after the restoration. Additionally, Lee (1999) and USACE (1998) planning sketches were hand-digitized. The radius of curvature, meander wavelength, amplitude, and arc angle were measured manually using a ruler, compass, and protractor for these data as well as the fieldwork and LiDAR data.

### **USACE documents and the HEC-RAS model**

A Freedom of Information Act (FOIA) request filed with USACE for documents related to the Pacifica stream restoration returned over 700 pages of engineering research and planning documents, including information on groundwater, contours, alternate plans, SPC custom regional curves, EIS/EIR reports, documentary photographs, and their preliminary flood model developed in HEC-RAS with cross-sections and associated high-resolution LiDAR data.

The original LiDAR data from Towill, the survey contractor for the cross-sections used in the flood model, was flown to augment data needs in the inaccessible portions of the

study area such as backyards (Towill 2011). This study uses the LiDAR ground-classified points (Figure 13) to create hand-digitized breaklines of the active channel and to investigate characteristics of the flood plain not visible in aerial and satellite imagery due to the dense vegetation. The submeter accuracy available for the reach allowed visualization of study area tributaries and secondary channels, as well as the initiations of chute cut-offs. Creating a route along the streams derived from the DTM allowed the creation of a longitudinal profile using LiDAR-derived elevations. This longitudinal profile is compared to fieldwork-derived profiles from 2003, 2005, 2007, and 2011.

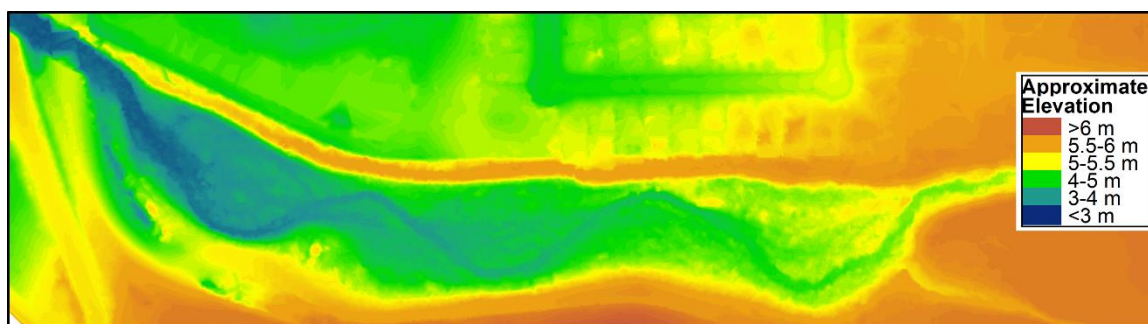


Figure 13: High resolution LiDAR flow in 2011 by Towill.

USACE's preliminary HEC-RAS flood model, which is subject to modification before their final summary of the project, includes four scenarios: two versions of the Highway 1 Bridge (as-is and renovated) and two sets of Manning's n values (design values and new proposed values). The stream variables involved in the model are discussed above, and the results of running the four scenarios are included below. The model was solved using all of the inputs and parameters as it was delivered. Variables extracted from the model are used to compare with other stream reach variable values. Furthermore, two of the contractor cross-sections from the HEC-RAS model were near this study's fieldwork cross-sections and are included for comparison.

### **Documentary photography**

Photographs from 2007, 2011, 2013, and 2014 are located along the stream by comparing details with 2014 geo-coded photographs. Additionally, photographs from USACE and other researchers are included and located with reference to the geo-coded 2014 photographs. The images are enlisted to build a theory of channel changes over time.

### **Daily precipitation data**

The annual maximum daily rainfall provides a rubric for comparing four local weather stations near SPC. Data for recent years at one Pacifica station were only available in fiscal year totals (July to June) and not in calendar year (January to December) or water year (October to September). Daily totals for some years were not available either. Therefore, because monthly and daily values were available at the other stations, annual values were all converted to fiscal year for comparison. Daily values for the three stations in Pacifica are compared with annual values from all four stations. Return intervals (RI) were also calculated for annual maximum daily storms for each station. First maximum daily precipitation values for each year were selected, then the events were ranked in descending order of magnitude, and finally RI was calculated such that  $RI = (n + 1) / m$ , where n is the number of years of data and m is the rank of the storm event. Then trendline equations to predict the storm return intervals for precipitation events, and vice versa, are reported for each of the weather stations. The return interval for the largest storms of 1982, 2005, and 2008 are calculated and compared by station as well. Finally a nearby gauged creek is assessed for its discharge and precipitation magnitude correlation.

With the lack of gauge data for the stream, annual maximum daily precipitation and storm return intervals are explored as proxies for predicting discharge and flood event return intervals. In particular, correlating known peak flow flood events with local precipitation data allows an analysis of the accuracy of this correlation.

## RESULTS

The results below include comparisons of remote sensing imagery and field data over time, a discussion of LiDAR contributions to fieldwork, and a summary of various meander variables related to the restoration process. Results of the USACE flood model scenarios are also presented, followed by documentary photography and a discussion of meander and bedform changes on the stream reach.

### **Vegetation observations**

Native plants observed in the 2007 and 2011 fieldwork included unidentified willows and alders, likely including the pre-restoration community (USACE and CP 1998) of shining willow (*Salix lucida ssp. ladiandra*), arroyo willow (*Salix lasiolepis*), Sitka willow (*Salix sitchensis*), and red alder (*Alnus rubra*). Other natives observed included California blackberry (*Rubus ursinus*), horsetail (*Equisetum*), native rushes (including *Juncus balticus*), California figwort (*Scrophularia*), and cow parsnip (*Heracleum lanatum*). These native plants were consistent with the scrub-shrub wetland and forested wetland planting schemes of the ecological restoration. Also found was an abundance of invasive pampass grass (*Cortaderia jubata*), watercress (*Rorippa nasturtium-aquaticum*), and Cape Ivy (*Delairea odorata*), along with some horticultural varieties presumably recruited from backyard gardens upstream (e.g. periwinkle (*Vinca minor*)). Finally, blue gum (*Eucalyptus globulus*) saplings were expanding into the floodplain and wetland area from the large stand uphill to the south.

As the stream bank vegetation has matured, the thick bank-stabilizing willows that were impenetrable in 2007 have opened up beneath the alder shade, modeling a natural succession. This delay to riparian forest was part of the design (Lee 1999). Eucalyptus seedlings were unnoticed in 2007, but by 2013 at least six saplings appeared in the FCP. The willows and alders are supplying woody debris to the stream reach, which is

beneficial for dissipating flow and providing salmonid habitat in scour pools where woody debris collects. The sprinkler infrastructure, installed to water the restoration vegetation for the first years, remains. Though abandoned, it offers convenient control points for stream surveys.

### Precipitation and flooding

San Francisco Airport (SFO), over a ridge to the east, and the three stations in Pacifica (locations shown in Figure 14) show a within region precipitation distinction, where the coast side of the ridge receives more rainfall than SFO. Pac-2, which is in Pacifica but outside of the SPC watershed, receives less than Pac-4 and San Pedro Valley Park (SPVP). Daily rainfall data (Figure 15) at SPVP indicate that 1982 had the highest annual maximum daily rainfall. This was also the case at SFO (daily values not shown).

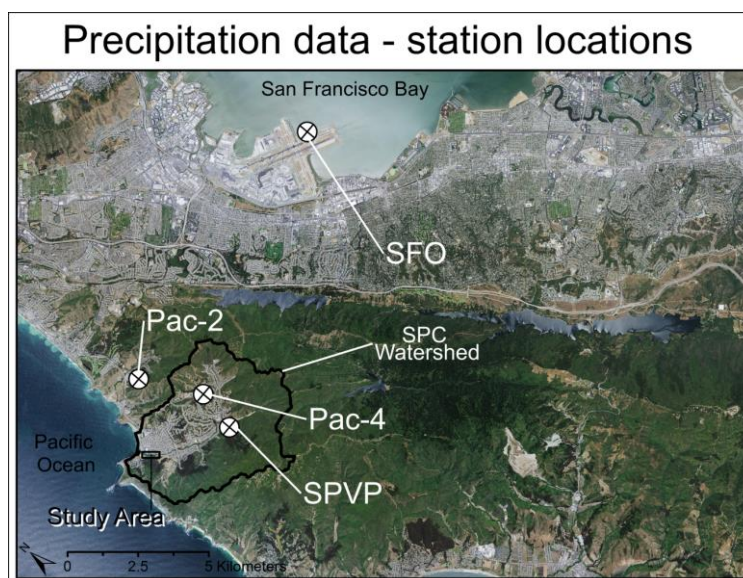


Figure 14: Precipitation data station locations. SPVP and Pac-4 stations are more indicative of precipitation in the SPC watershed than Pac-2 or SFO, which are outside the watershed.

Because SFO has longer term data, correlating SFO annual precipitation with SPVP annual precipitation (Figure 16) results with  $R^2=85\%$ . This SFO and SPVP correlation is used to extend the SPVP data in Figure 4.

Daily and annual rainfall are graphed together for the four stations in Figure 15. Although both SFO and SPVP daily records have the 1982 storm as their highest daily precipitation event, fiscal year 1983 had a higher annual total for precipitation than any other year on record for SPVP. Similarly, the January 25, 2008 peak flow event (circled in Figure 15) occurs in a lower annual precipitation year, and not one of the highest on record in Pacifica. The other two Pacifica stations (Pac-2 and Pac-4) began recording after 1982 and both have 2005 as their highest annual maximum daily rainfall event, which had an annual precipitation total slightly higher than the mean of 956 mm.

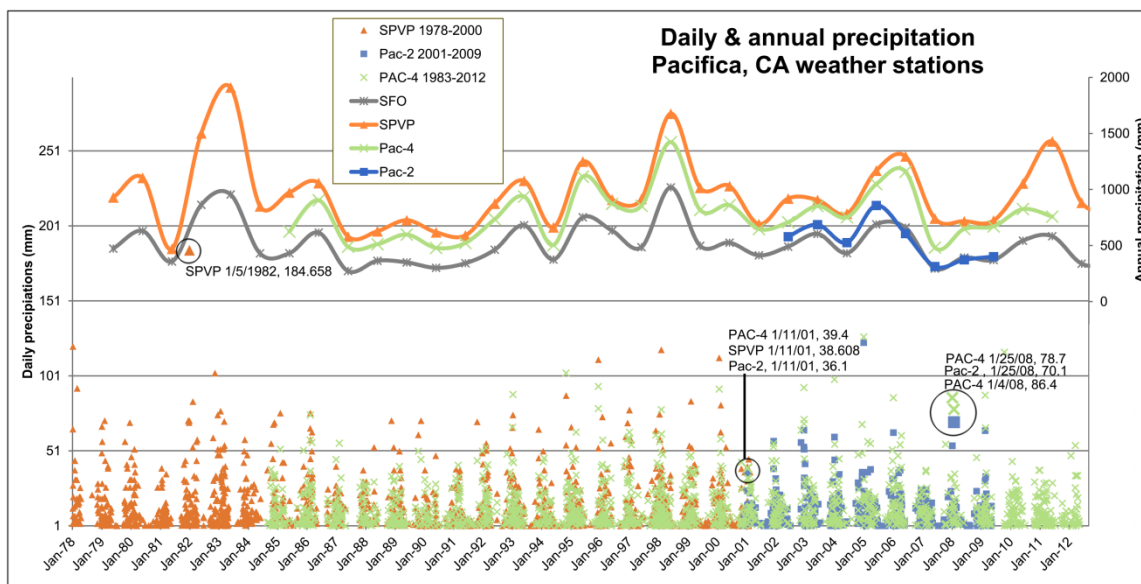


Figure 15: Daily rainfall 1978–2012 at three local Pacifica stations is compared to their annual precipitation and annual precipitation from SFO (daily SFO not shown). Data courtesy of San Pedro Valley Park and wrcc.dri.edu.

Because of the different lengths of annual data available, there are different return graphs for each station (Figure 17). SFO has the longest record of 63 years and so the 1982 storm event shows as a 64 year return interval storm. However, the SPVP station had only 23 years of data and therefore shows the same storm as a 24-year return interval storm. The trendlines for storm return interval per station are shown in Figure 18. These

are then used to calculate theoretical precipitation magnitude for the USACE return interval values of 1, 2, 5, 10, 25, 50, and 100 years (Table 2).

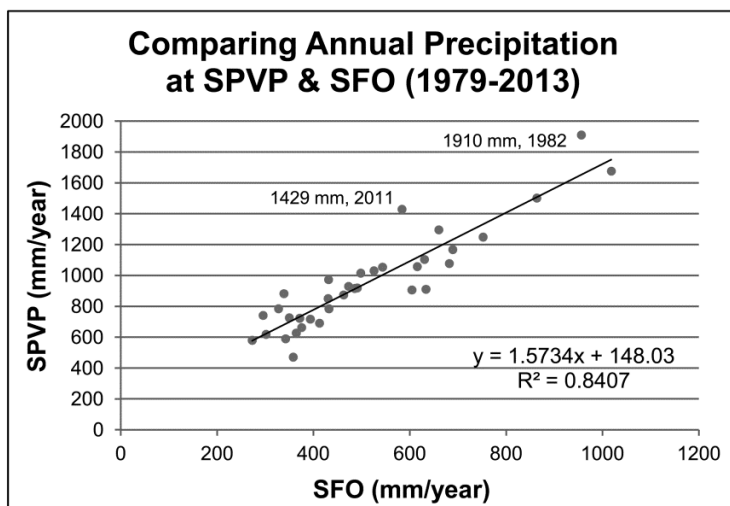


Figure 16: Correlating annual precipitation at SFO and SPVP. Data courtesy of San Pedro Valley Park and wrcc.dri.edu.

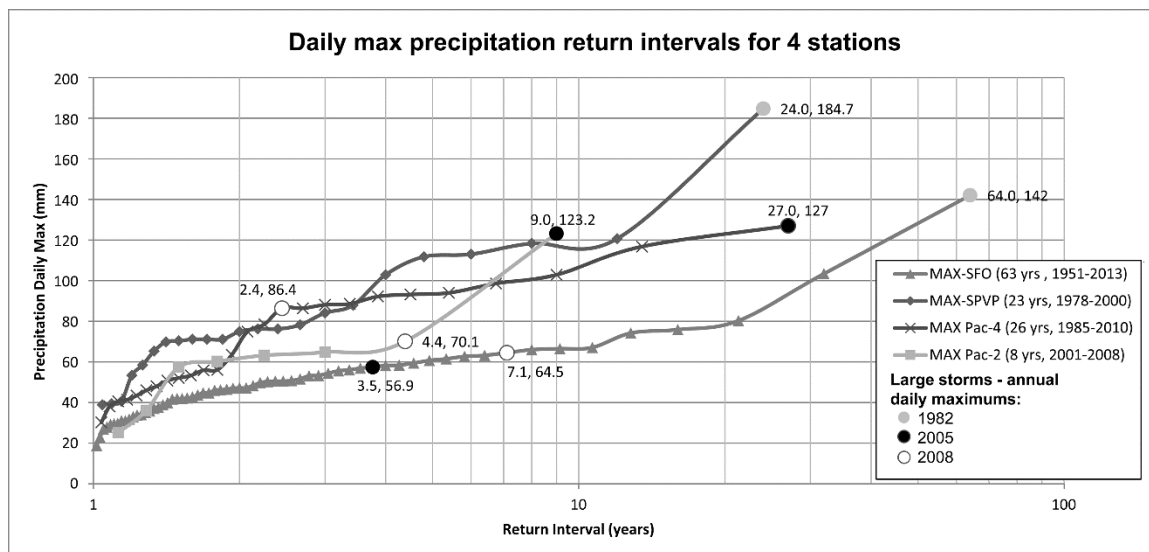


Figure 17: Annual maximum daily precipitation return intervals for four precipitation data sets, including three in Pacifica and one at SFO. Same day largest storms for 1982, 2005, and 2008 are labelled with return interval (years) and precipitation (mm). Data courtesy of San Pedro Valley Park and wrcc.dri.edu.

Return intervals for the storms in 1982, 2005, and 2008 are then calculated using the trendlines (Table 3). It is interesting to note that the 2008 storm in Figure 17, found in all but the SPVP dataset, ranges from a 2.4 to 4.4 year return in Pacifica and 7.1 year return at SFO. Calculating 2008 return intervals using the trendlines gives 2.9 to 4.3 in Pacifica and 5.5 at SFO (Table 3). These same three stations also captured the 2005 storm, which was the largest-on-record storm for the two Pacifica stations at 9- and 27-year return intervals. However, the SFO return interval was only 3.5 years. This may be an artifact of fewer years of data or demonstrative of a particular wind direction during the storm. The trendline return interval calculations for 2005 maximum event are 11.4 to 16.4 years in Pacifica and 3.8 years at SFO. Finally, the 1982 storm, captured by SFO and SPVP, has return intervals of 64 and 24, respectively, being the maximum event on record. However, the trendline calculations return 246.4 years for SFO and 37.7 years for SPVP. This is not surprising, given the steep slope of the SPVP trendline and the low slope of SFO. Nevertheless, it shows the difficulty in assessing return intervals with limited and varying years of precipitation data.

It is noteworthy that the 2008 peak storm event was only slightly larger than an average maximum storm. This storm produced a peak flood, which may have had a larger return interval than the storm due to the fact that weeks before, on January 4, 2008, there was a similarly high daily precipitation event (shown in Figure 15), which would have increased the antecedent moisture content and contributed to the peak flow event.

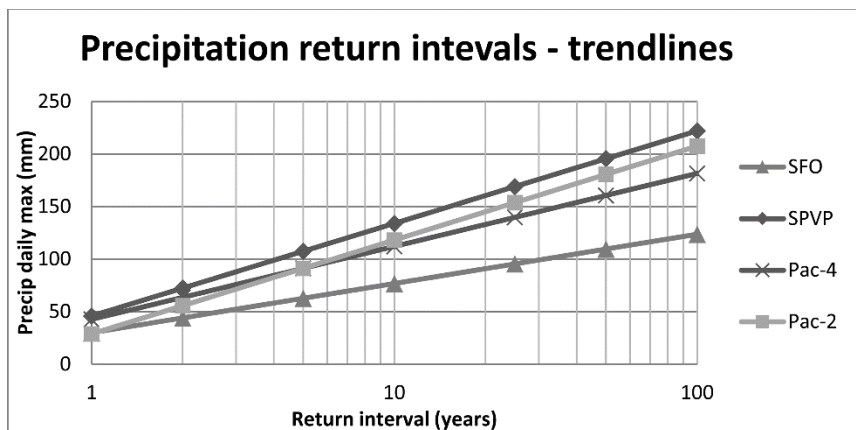


Figure 18: Precipitation return interval trendlines with points at return intervals for years 1, 2, 5, 10, 25, 50, and 100.

Return Interval (yrs):	1	2	5	10	25	50	100	Equation to calc precip:
SFO (mm)	30	44	63	77	95	110	124	$y = 20.34 \ln(x) + 29.99$
SPVP (mm)	46	72	107	134	169	196	222	$y = 38.24 \ln(x) + 45.95$
Pac-4 (mm)	43	64	91	112	140	161	182	$y = 30.13 \ln(x) + 42.73$
Pac-2 (mm)	29	56	91	118	154	181	207	$y = 38.80 \ln(x) + 28.82$

Table 2: Calculated precipitation for various return intervals of annual maximum daily precipitation, given the trendlines in Figure 18.

Year:	Max Precip (mm)			Ret Int (yrs)			Equation to calc return int:
	1982	2005	2008	1982	2005	2008	
SFO	142	56.9	64.5	246.4	3.8	5.5	$y = e^{(x-29.99)/20.34}$
SPVP	184.7	-	-	37.7	-	-	$y = e^{(x-45.95)/38.24}$
Pac-4	-	127	86.4	-	16.4	4.3	$y = e^{(x-42.73)/30.13}$
Pac-2	-	123.2	70.1	-	11.4	2.9	$y = e^{(x-28.82)/38.8}$

Table 3: Calculated return intervals for the storms in 1982, 2005, and 2008, given the trendlines in Figure 18.

There are few dates available to compare all three Pacifica stations, but January 11, 2001, does overlap them all (Figure 15). It is interesting to note that SPVP had a lower daily value than Pac-4, but higher than Pac-2. The SPVP and Pac-4 overlap of daily precipitation values (orange triangles and green crosses) shows that higher rainfall values (over 50 mm in one day) rarely coincide with both stations getting a peak storm event. This is likely due to storm path variability and local topographic differences in weather station locations (Figure 14). However, SPVP consistently had higher annual

precipitation totals as compared with both Pac-2 and Pac-4. This is consistent with Amato (2003), who suggested that there was a substantial gradient of rainfall increasing south through Pacifica towards Montara Mountain.

The range of storm return interval values for the same year's storm compounds the difficulty in estimating the flood return intervals. Even with discharge information, correlating storm magnitude with discharge magnitude is complicated due to variables not assessed in this study such as antecedent moisture content and basal flow.

The 1982 flood inundated 0.69 km<sup>2</sup> of the business and residential area to the north of SPC FCP. USACE and CP (1998) estimate the peak stream discharge related to the January 1982 storm to be 81.8 m<sup>3</sup>/s on San Pedro Creek at Linda Mar Bridge, noted as a watershed of 20.7 km<sup>2</sup>. Using the USACE discharge rating curve in Lee (1999) for FCP, just downstream, we see that it was a 40-year return interval flood event. This is comparable to the Table 3 storm return interval value (37.7) for the 1982 storm at SPVP.

Nearby coastal stream gauges recorded the 1982 peak discharge values as 224 m<sup>3</sup>/s (San Gregorio Creek, 131.8 km<sup>2</sup> watershed), 266.2 m<sup>3</sup>/s (Pescadero Creek, 119 km<sup>2</sup> watershed), and 134.5 m<sup>3</sup>/s (Pilarcitos Creek, 70.4 km<sup>2</sup> watershed). The flood return interval on San Gregorio Creek, 32 km to the south of San Pedro Creek, was 39 years for the 1982 flood. This was the highest interval possible with 38 years of discharge data. In fact, both the 1982 discharge event and the associated 1982 precipitation event were ranked number one in magnitude during the period of records. However, San Gregorio Creek discharge and precipitation were not always ranked equally for the same discharge and storm events (Figure 19). The annual maximum daily discharge and precipitation ranks for 1982 and 2005 are comparable, but 9 of the 27 precipitation ranks are further than 5 away from the associated discharge rank, which would lead to an even wider discrepancy of calculated return interval values.

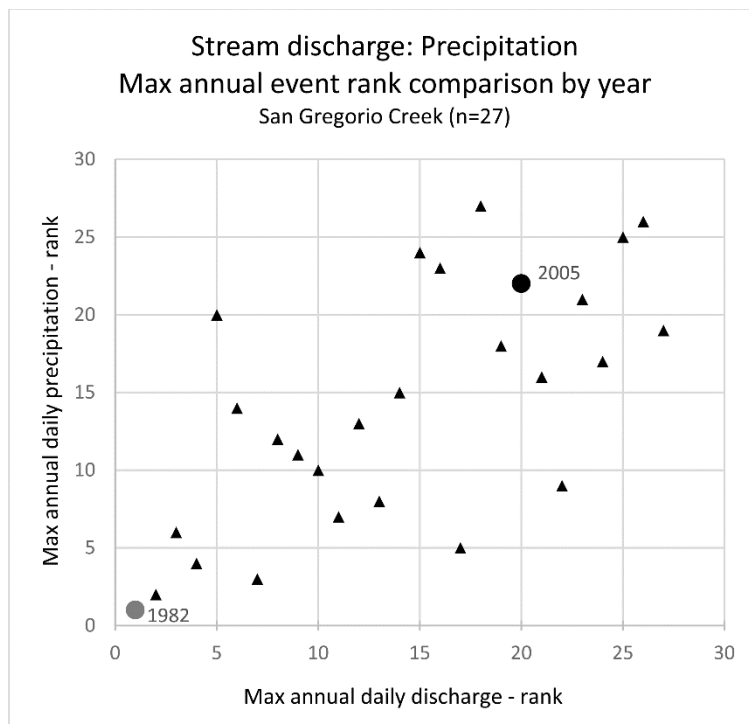


Figure 19: San Gregorio Creek discharge and precipitation correlation. Annual peak daily discharge ranked by magnitude is compared to the same year's annual maximum daily precipitation ranking by magnitude. Stream gauge data from [nwis.waterdata.usgs.gov](http://nwis.waterdata.usgs.gov) and precipitation data from [weather-warehouse.com](http://weather-warehouse.com).

### Remote sensing and planviews

Aerial imagery of the stream reach from 1993, 2002, 2005, and 2011 illustrate the planform development of the restoration process (Figure 20). Figure 20A shows the pre-restoration stream reach in 1993 as a linear riparian stretch across the middle. Figure 20B shows the restoration in progress in 2002, with the original channel intact and the restoration channel's first dig before stream re-routing. Figure 20C shows the completed restoration channel in 2005, the new earthen berm replacing the old channel, and the success of vegetation irrigation. Figure 20D shows the dense vegetation in 2011 mostly obscuring the channel, which made the LiDAR data invaluable for channel delineation.

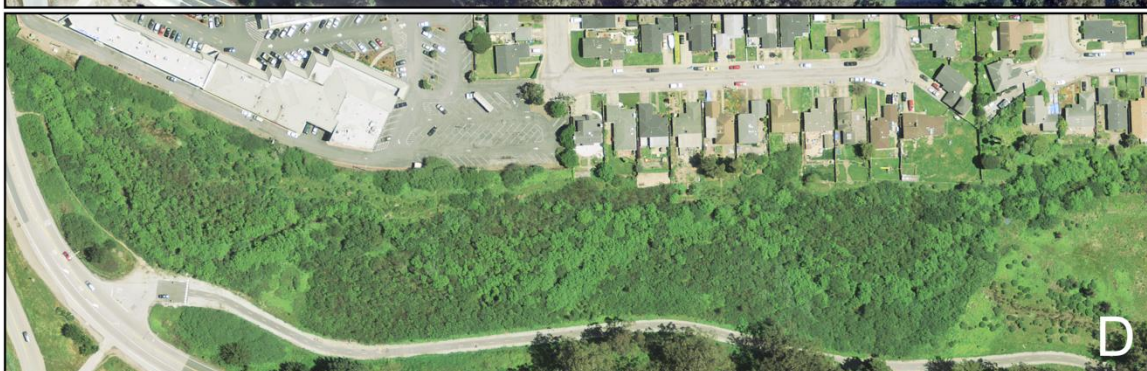
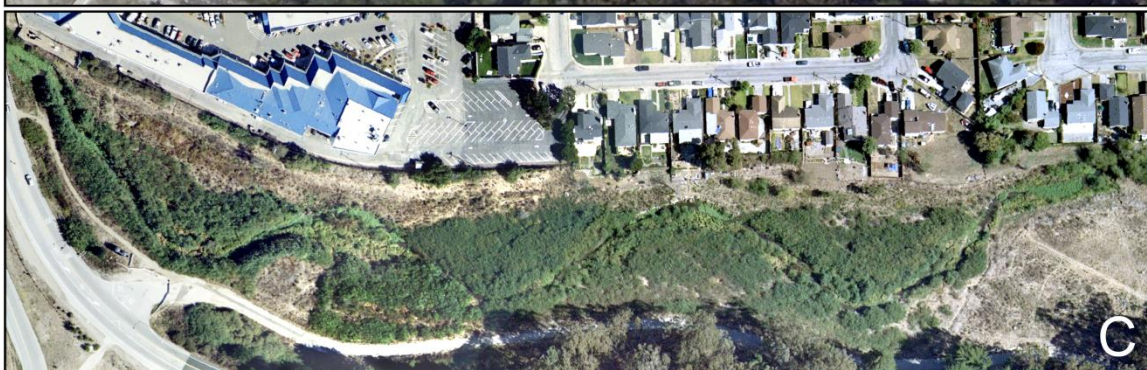
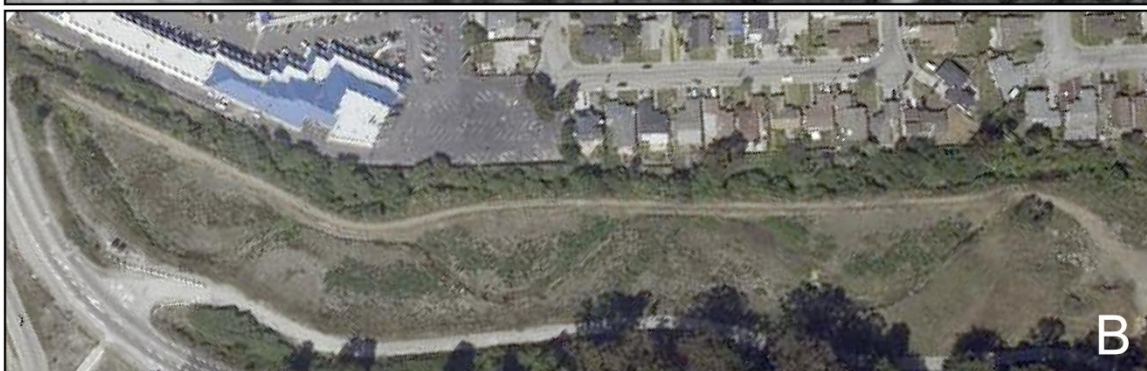


Figure 20 (previous page): USGS high-resolution aerial orthoimagery of the stream reach over time. **A: 1993** (DOQQ 30 cm resolution), **B: 2002** (MrSID 30 cm maximum resolution), **C: 2005** (seamless 15 cm resolution), and **D: 2011** (seamless 30 cm resolution)

Hand-digitized planview data are collected and presented for comparison in Figure 21B. The 2011 LiDAR data (Figure 21A) were used to derive streams and hand digitize streambed breaklines (Figure 21C). These are compared to the other data sources, including fieldwork planforms (Figure 21C thalwegs), hand-digitized design planforms from the planning documents from USACE's original sketch (1998) and Lee's (1999) approved design. These differ from the as-built installed restoration first dig.

Digitized planforms representing the meander design sketches and the implementation process illustrate differences among the designs and the as-built. USACE (1998) used four meander pairs (eight bends), where Lee (1999) sketched three pairs (six bends) (Figure 21B). The digitized rendering of the stream channel reveals that Lee's design is also different from the as-built 2002 first dig and the 2011 channel, which were digitized from orthoimagery. The change from Lee (1999) was in order to preserve an Ohlone shellmound uncovered during construction (Ungvarsky 2002).

Planviews of the stream reach for the thalweg surveys in 2007 and 2011, and for the 2011 LiDAR-derived streams (Figure 21C), show a relatively unchanged meander geometry during 2007 to 2011 on the coarse meander scale. The LiDAR derived streams in white show headcutting onto the stream banks at inflection points between meander bends (Figure 21C). This is also visible in the LiDAR elevation raster (Figure 21A), particularly at the point labelled "side channel" in Figure 21C.

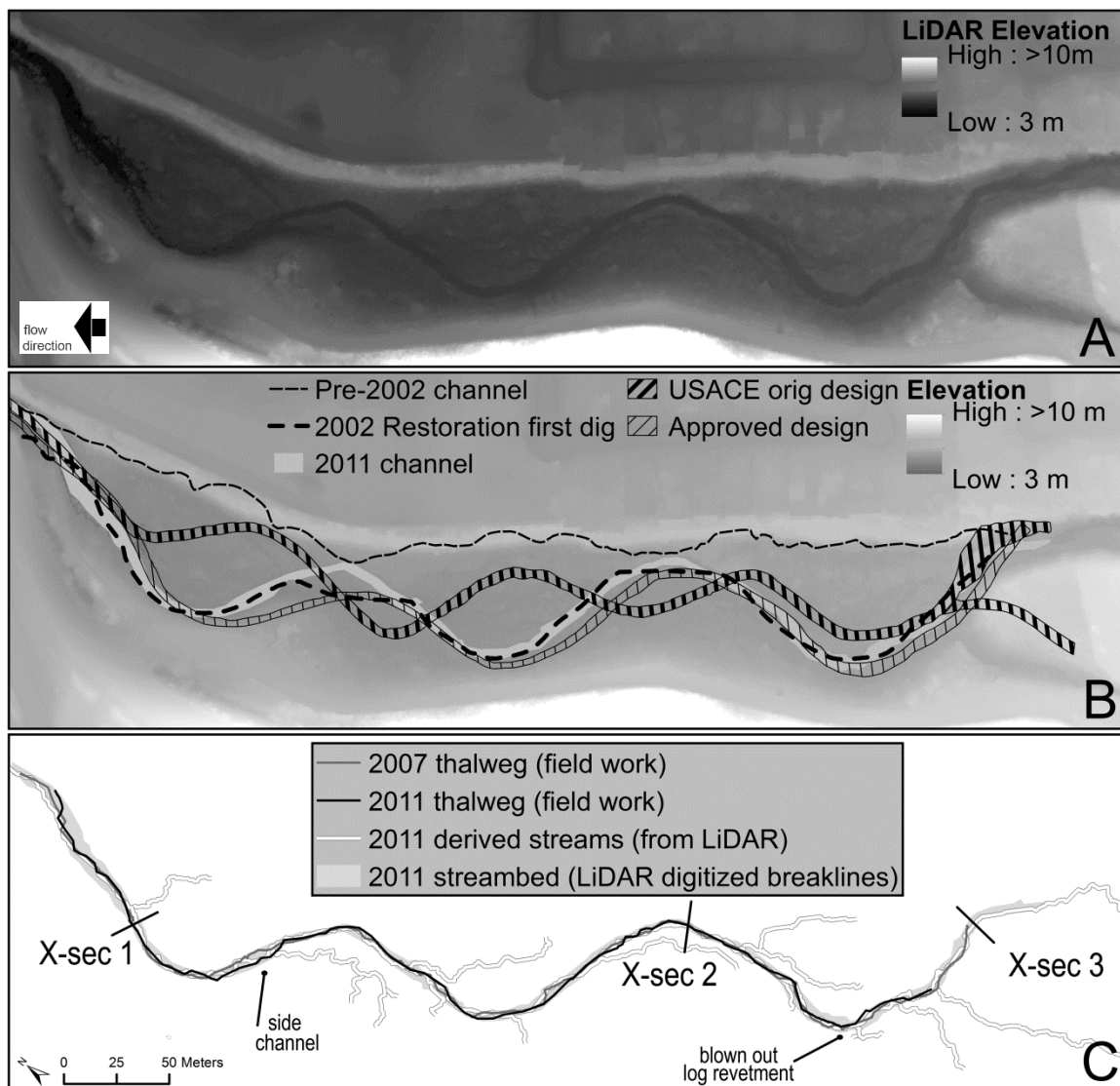


Figure 21: Planviews comparing LiDAR and other data sources. A: LiDAR planview of the stream reach, B: Planviews digitized from sketches and orthoimagery, and C: Planviews of fieldwork (2007 and 2011) and LiDAR derived streams, along with digitized stream channel breaklines. The culvert draining in to the study area from the lower right, shows clearly in A.

### Meander planform variables

Simplified planviews for all data sources are presented in Figure 22. To better visualize the details of each data source, the stream reaches derived from data sources are positioned in a single layout with the data source label located along the right margin.

Points were placed by visual inspection at points of concavity change. The bedform variables, measured from randomly selected segments from the 250–400 m range of the scale bar for each data source, are presented in Table 4. Each data source provides different resolution of detail. For example, the fieldwork scale of the thalweg moving from bank to bank has a finer resolution than the simple line drawing of the designed meander. The 2011 LiDAR breaklines shows the hand digitized streambed.

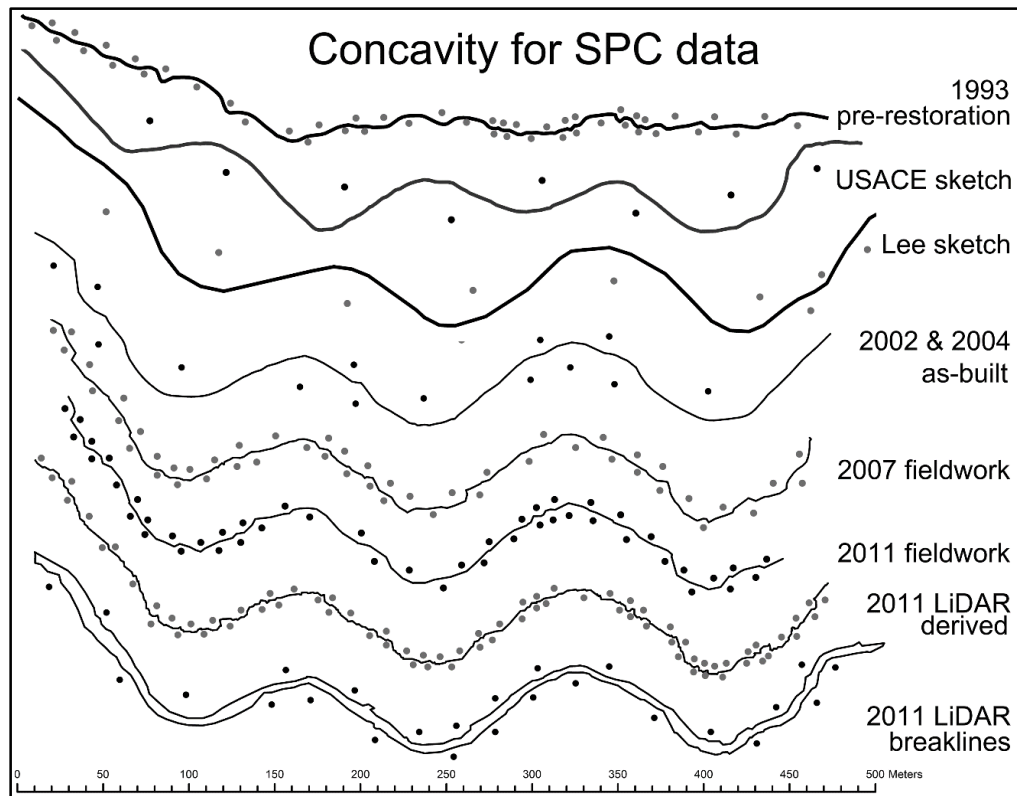


Figure 22: Concavity changes were noted visually and indicated with points. Each data source is labelled at right.

Year:	1993	1998	1995	1999	2002 & 2004 As-built	2004 As-built	2007	2011	2011	2011	2011
Source:	DOQQ	USACE sketch	Lee forms	Lee sketch	ortho- imagery	Davis (2008)	fieldwork	fieldwork	HEC-RAS	derived	breaklines
Reach Length (m)	519.7	595.6	597.4	622.1	583.1		598.8	537.6	638.8	659.6	623.2
Linear Lenth (m)	473.8	502.2		504.7	467		454.8	426.7	522.3	467.2	494.3
Sinuosity	1.1	1.19	1.33	1.23	1.25		1.32	1.26	1.22	1.41	1.26
Slope	0.0044*		0.3				0.0029	0.003	0.0038	0.003	0.003
Bankful width (m)	6.6 *		15.24				11.3		47 (2-yr@CS2)		
W/D ratio	4**		20				18.5		29.4		
Discharge (m <sup>3</sup> /s)			12.74 bf				0.019	0.039	19.8 (2-yr)***		
Rosgen Classification	E*		C4-C5	B4-B5			C4				
Radius of curv (m)	6.6	27.5	38.1	52.8	29.0	33****	13.2	17.6	55.0	8.8	20.0
Wavelength (m)	13.2	101.0	137.2	167.2	76.0	154.0	30.8	26.4	105.6	26.4	37.0
Amplitude (m)	3.3	27.0		47.3	7.5	43****	2.2	2.2	19.8	33.0	9.0
Arc Angle (degrees)	90	110		110	95	135****	60	38	63	70	30

\* Collins, Amato, & Morton (2001) - a 948 m survey  
\*\* USACE (1998)  
\*\*\* USACE (1998) has discharge value 12.75 for 1-year flood event (not included in HEC-RAS).  
\*\*\*\* Values are calculated from Davis (2008)'s wavelength diagram

Table 4: SPC FCP bedform and floodplain variable comparison for data sources.

Pool spacing measured in 2014 (Figure 23) between meander bend 1 at Highway 1 and bend 6 upstream was inconsistent, with closer spacing at and downstream of bend 5 and spacing increasing towards bend 1. There were no inter-meander pools between bend 5 and bend 6, which is consistent with theoretical pool riffle sequences. Between bend 1 and bend 3 the pool spacing was approximately 45 m. Between bend 3 and bend 5, the spacing decreased to approximately 35 m. Between bend 5 and bend 6, there were only two pools located at the meander bends themselves, specifically undercutting log revetments. At the same time, this reach had point bars near bend 5 and bend 6, but not between during 2005 to 2011. The pool riffle spacing values overall are lower than the range estimated by Davis (2008) and much lower than his reverse calculations from as-built meander wavelength to pool spacing. The point bars generally follow a shorter wavelength rhythm and not the designed meander and point bar wavelength proposed by Lee (1999).

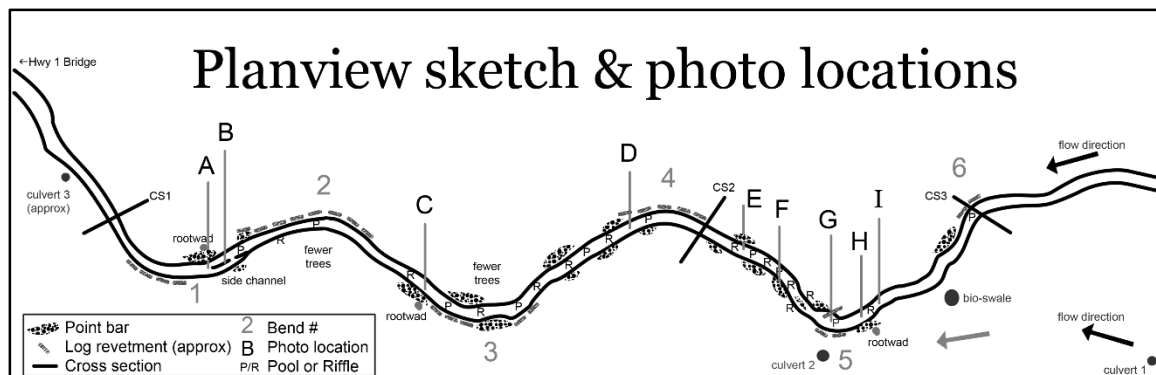


Figure 23: Planview sketch and locations of photographs (“A”, “B”, “C”, etc.) discussed later.

### Longitudinal profiles and cross-sections

The longitudinal profiles derived from fieldwork for 2003, 2005, 2007 and 2011 are shown in Figure 24. An average aggradation from 2003 to 2005, and a thalweg slope moving from 0.0032, to 0.0042, is followed by a trend of degradation from 2005 to 2007, with the slope moving down to 0.0029. There is then a trend of aggradation from 2007 to 2011, resulting in the slope rising slightly to 0.003, with the base level also rising slightly. Fieldwork in 2003 and 2005 followed the initial floodplain revegetation and channel rerouting, which possibly resulted in lower Manning’s  $n$  floodplain and channel values, increasing erosion downstream. However, deposition upstream actually filled in the channel slightly, resulting in net aggradation for that period. 2007 fieldwork followed two years of high rainfall, likely scouring the channel, despite the increased vegetation and roughness. 2011 fieldwork followed three (fiscal) years of lower annual rainfall (2008–2010), thereby possibly contributing to aggradation of the streambed. In 2014, it was observed that the lower reach had degraded, exposing irrigation pipes within the stream bed installed in 2002, which were also noted in 2007.

The 2011 longitudinal profile is compared to the LiDAR-derived streams (Figure 25). However, the LiDAR return points that penetrated the water surface were removed by Towill (2011) when preparing the data for delivery.

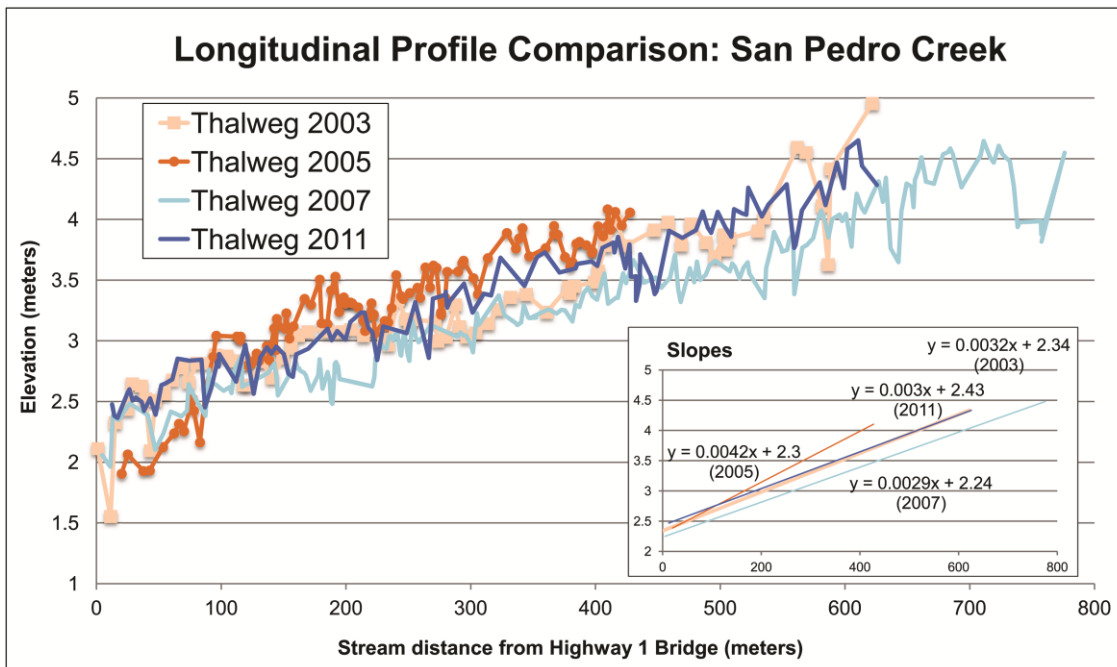


Figure 24: Longitudinal profile comparison I: Fieldwork in 2003, 2005, 2007, and 2011, with inset trendlines.

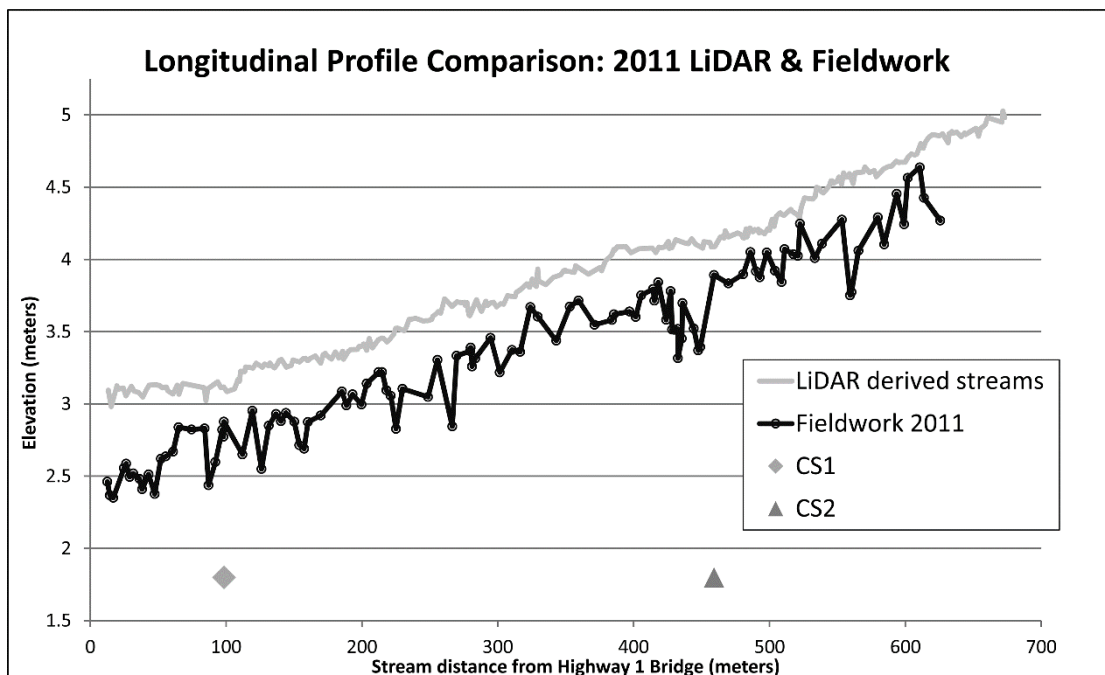


Figure 25: Longitudinal profile comparison II: LiDAR derived streams from March 2011 is compared to the fall 2011 data. Approximate location of CS1 and CS2 are shown.

The 2011 fieldwork longitudinal profile graphed in Figure 25 has a transformation of the elevation values shown in Figure 24 to adjust for different bench mark standards between the LiDAR and fieldwork. Fieldwork points are relative to the bench mark disc Y1240 placed in 1972 for the U.S. Geodetic Survey on the Highway 1 Bridge crossing SPC FCP and noted by previous researchers as having elevation 4.39674 m. However, the bench mark disc has elevation of 5.043 m using the vertical datum NAVD88 (Groundspeak 2015), which is the datum that the Towill LiDAR and ground survey used (Towill 2011). In order to graph the 2011 field data with the 2011 LiDAR data, therefore, the field data points have an elevation translation of +0.64626 m,. Unfortunately, with the Highway 1 Bridge reconstruction in late 2014, this bench mark was removed (Groundspeak 2015) and will therefore not be available for future studies.

There were three repeated cross-sections. Note that y-axis values for the cross-section graphs do not relate to elevation but are instead relative only to the cross-section years being compared. Also note that the left bank (LB) is on the left when looking downstream. CS1 (Figure 26) repeats the longitudinal profile results of degradation from 2004 to 2007 and aggradation from 2007 to 2011, showing a 0.38 m drop in streambed elevation followed by a 0.33 m rise. The corresponding water levels (positioned on the y-axis for comparison) also display this pattern. The HEC-RAS data available near the fieldwork cross-section is included below and shows both the 2-year and 100-year water surface level (WS).

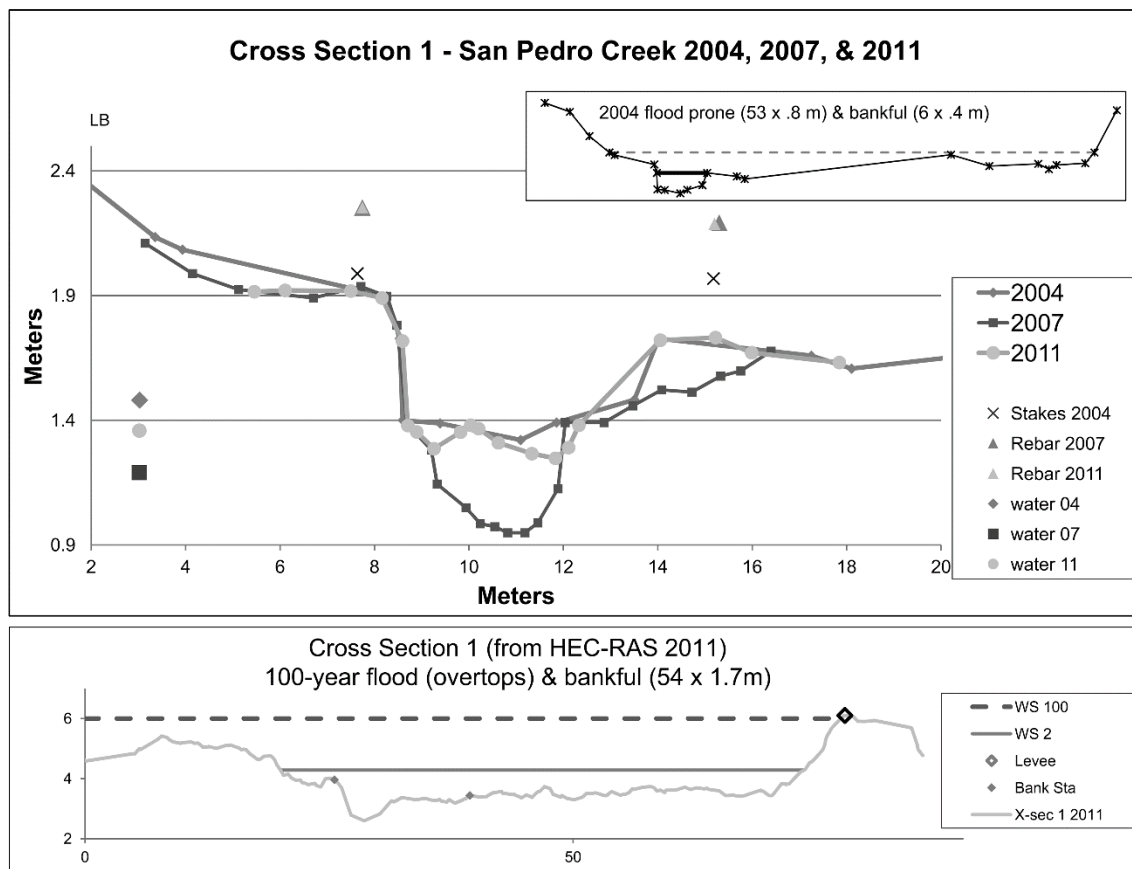


Figure 26: Cross-section 1 (CS1) showing data from 2004, 2007, and 2011, along with USACE HEC-RAS data from 2011 (lower graph). The above graph shows water levels near the y-axis for each year and includes cross-section benchmarks stakes and rebar. The lower graph shows water level for 2 year and 100 year flood levels (WS 2 and WS 100) as well as bankfull field indications (Bank Sta). See Figure 21C and Figure 23 for cross-section location.

CS2 (Figure 27), on the other hand, maintains its streambed elevation. This is due to pre-restoration erosion-resistant materials, either Quaternary clays or bedrock exposed in the streambed (Figure 28). Clays would be explained by 1989 soil boring that found peat or peaty clay 1.8–3 m below the surface in three boring holes on SPC FCP, providing evidence of previous wetlands on the site (Lee 1999). Note that the water levels for 2007 and 2011 at CS2 are identical. However, up on the left bank shows erosion under the rebar, while the right bank shows some aggradation similar to that in CS1 from 2007 to 2011.

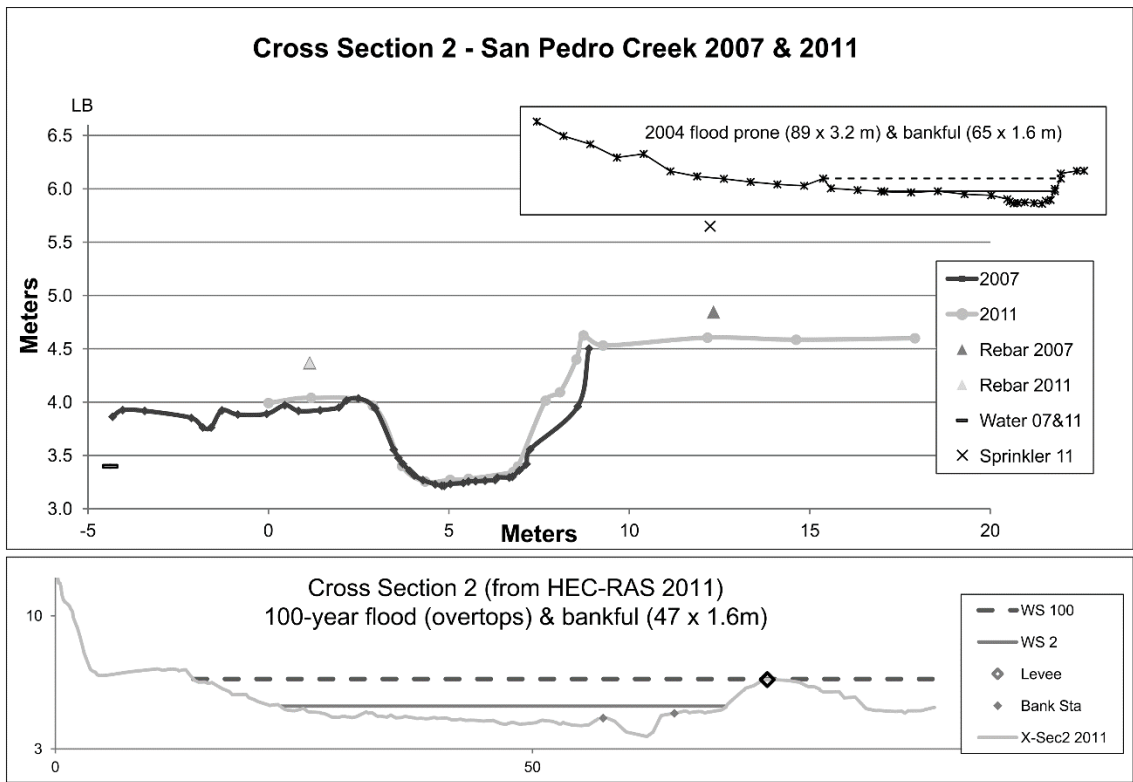


Figure 27: Cross-section 2 (CS2) showing data from 2007 and 2011, along with USACE HEC-RAS data from 2011. The above graph shows water level near the y-axis and includes cross-section benchmarks rebar and sprinkler. The lower graph shows water level for 2- and 100-year flood levels (WS 2 and WS 100) as well as bankfull field indications (Bank Sta). See Figure 21C and Figure 23 for cross-section location.



Figure 28: Either bedrock or erosion-resistant Quaternary clays located downstream of CS2 at photo location "D".

CS3 (Figure 29) captures a deep pool near the uppermost extent of the study area at bend 6. There was undercutting of the log revetment on the right bank not fully illustrated in the cross-section due to limitations of delineating the underbank contour with the digital level. The pool aggraded slightly from 2007 to 2011, while the steep left terrace eroded the prior bankfull rounded morphology into a steep slope.

The lower graphs of CS1 and CS2 show 2- and 100-year-flood extents modified from USACE HEC-RAS flood modeling. CS1 shows an overtopping towards the leftbank floodplain (Figure 26) at the 100-year level. This overtopping occurs in the 50- and 100-year models using either the as-is Highway 1 Bridge or the new proposed bridge, along with the proposed Manning's n values. However, the leftbank direction leads to a steep rise to the south and may not imply a flooding hazard. Longer cross-sections are needed to model this outcome. However, the CS2 HEC-RAS 100-year flood level overtops the right bank earthen berm into a residential area (Figure 27 lower graph). This cross-section breaches the right bank berm with both bridge models and using the proposed Manning's n value, but only at the 100-year flood level. The model is still preliminary, and needs further analysis.

Pebble counts were taken at cross-sections only and do not characterize the full breadth of riffles, runs, and pools in the reach (Figure 30 and Figure 31). However, CS1 was a riffle, while CS2 was a run and CS3 was a pool. The D50 of the three cross-sections shifts from medium gravel (8–16 mm) in 2007 to very fine gravel (2–4 mm) in 2011. The D83 values on the reach shifted slightly from 2007 to 2011, decreasing from very coarse gravels (32–64 mm) to coarse gravels.

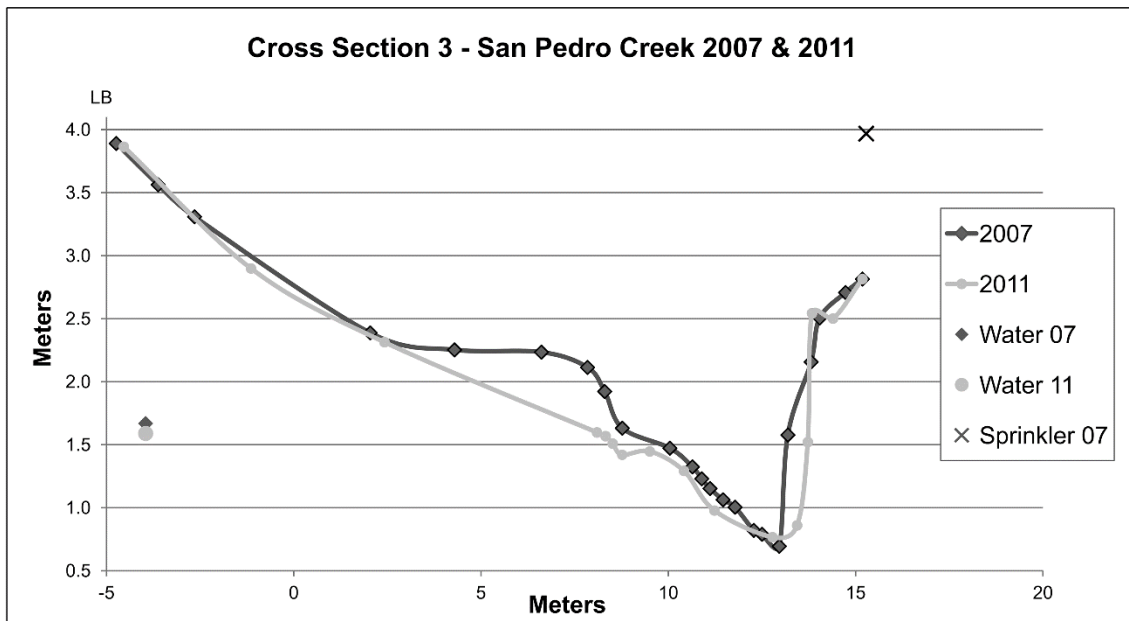


Figure 29: Cross-section 3 (CS3) comparison for 2007 and 2011. The graph shows water level for each year near the y-axis and includes benchmark sprinkler. See Figure 21C and Figure 23 for cross-section location.

At CS1 the local D50 shifts down from medium gravels in 2007 to fine gravels (4–8 mm) in 2011. Similarly at CS2 there was a decrease in D50 size from coarse gravel (16–32) to fine gravels. And finally at CS3 the shift down is from fine gravel to sand (.062–2 mm). Note that in 2007, there was not a category for silts and fines (graphed in 2011 as 0.1 mm) and were included in the <2 mm category. This did not affect the D50 values, however.

At and downstream of CS2 there were more hard clays than in other part of the study area, due to eroding into older pre-restoration deposits. This area also had no point bars. At CS3, there were finer sediment sizes due to it being a deep pool.

In comparison, the D50 class from Collins, Amato, and Morton (2001) for the reach is fine gravel (18%), which is the same class as the 2011 values. Collins et al. (2001) also found less than 4% silt and clay (<0.062 mm) on the SPC FCP reach, with 24% sand,

11% very fine gravel, and 42% medium, coarse, or very coarse gravel (8–64 mm). The D83 value in 2001 was coarse gravels, which is also the same as the 2011 pebble count value for the reach.

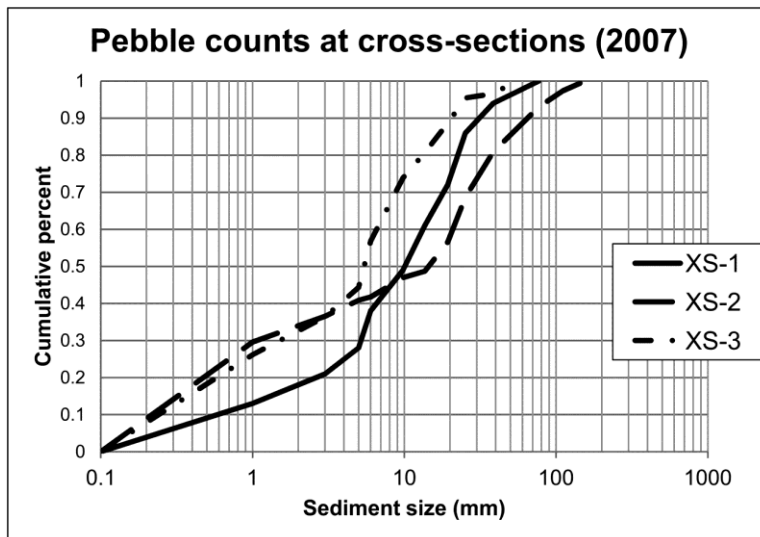


Figure 30: Pebble counts for 2007 at the cross-sections only. XS-1 is CS1 or cross-section 1. Similarly XS-2 is equivalent to CS2 and XS-3 is equivalent to CS3.

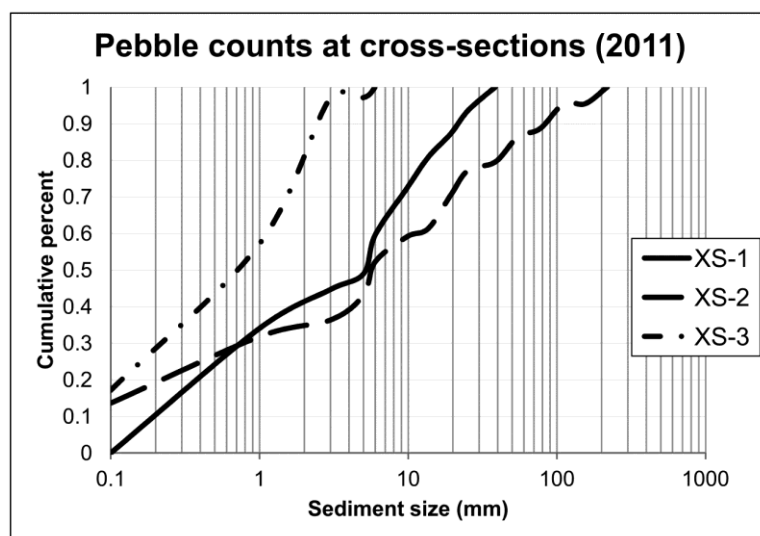


Figure 31: Pebble counts for 2011 at the cross-sections only. XS-1 is CS1 or cross-section 1. Similarly XS-2 is CS2 and XS-3 is CS3.

**HEC-RAS flood model**

HEC-RAS modeling showed levee overtopping just upstream of the Highway 1 Bridge for the model scenarios with the as-is bridge at the 100-year flood level. For the USACE proposed Manning's n values with the as-is bridge, overtopping occurred at the Highway 1 Bridge at a 50-year return interval flood and at five other cross-sections along the leftbank. At the 100-year level with the as-is bridge and the proposed Manning's n, there were also two overtoppings near cross-section 2 and one at the upstream end of the reach (Figure 32). For the proposed new bridge and proposed Manning's n values, the 50-year return interval flood reaches the extent of the model only in three of the leftbank cross-sections. However, the 100-year flood extends to the model limit for six leftbank cross-sections, along with the two near CS2 and the one at the upstream end. However, it does not overtop at the bridge at the 100-year level. To will digitized the bridge designs and provided the survey cross-sections to USACE for the HEC-RAS model (USACE 2013). With the new bridge completion due in 2015, the model will have to be updated using the as-built design.

The two middle arrows (of the four in Figure 32) are near the residential area of CS2 shown in Figure 33. The location of CS2 on the reach is shown in Figure 23. Residential fences are visible at the top left and log revetments line the right bank until midframe where the revetments are set back from the stream, covered by material eroded down from above. This area, along with the Highway 1 reach, the leftbank, and the upstream end, are the primary area of concern for flood hazard as predicted by the HEC-RAS flood model.

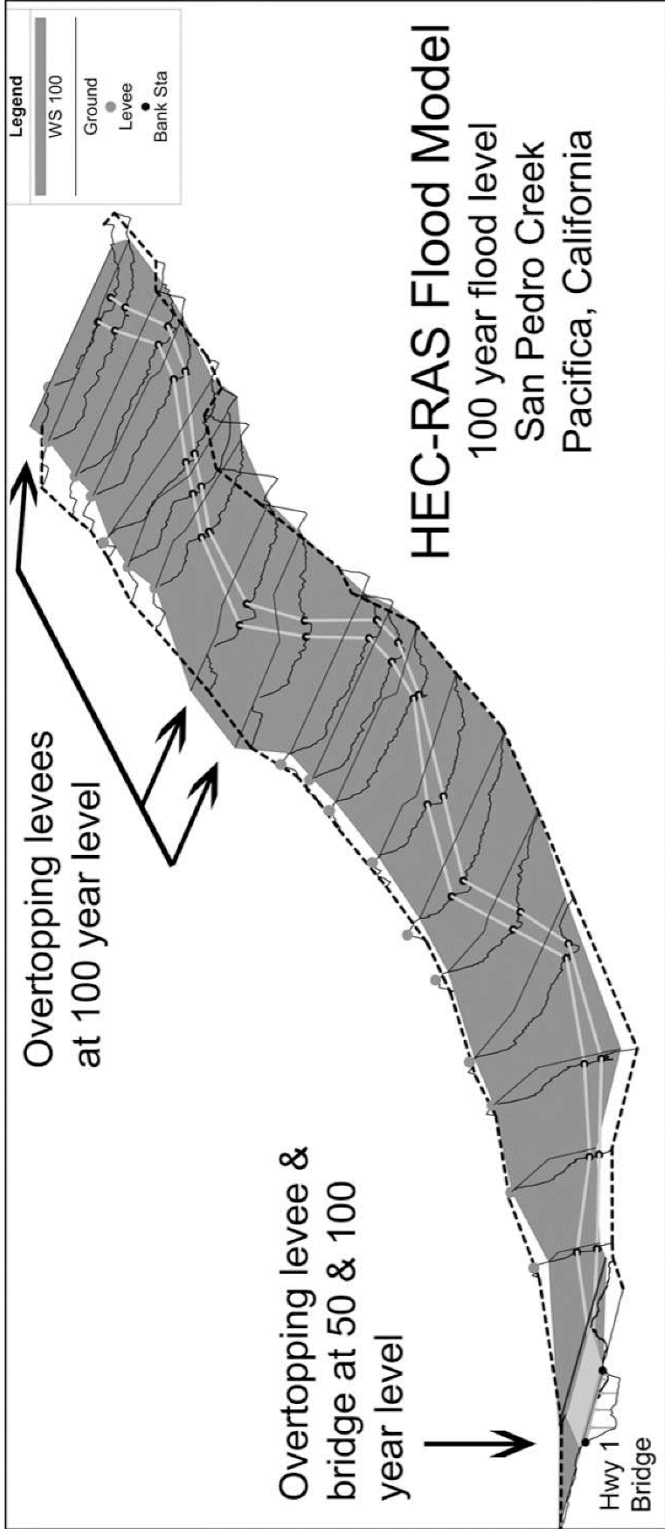


Figure 32: HEC-RAS model result for 100-year flood level. Water surface (WS) overtops levees at Highway 1 for the 50- and 100-year flood return levels with the as-is bridge and proposed Manning's n values. The berm near CS2 and the berm at the upstream extent of the model both overtop for the 100-year flood level for the proposed Manning's n values and both the as-is bridge or the new bridge. Left bank overtopping near CS1 and elsewhere are not visible in this diagram but are also present for both bridge scenarios.

Note that the stream is delineated in white while the cross-sections and associated water surfaces are in black. The dashed lines show the full extent of the model width.

### **Meander adjustments**

Documentary photography of the meander reaches helps to explain some of the study area's geomorphologic adjustments to the restoration. The following sections explore meander dynamics on the reach. First, designed point bar spacing and patterns are assessed. Second, backwaters at an inflection points between meander bends precipitates headcutting towards a chute-cut off. Third, three vertical logs originally delineating the stream bank of the active channel are now behind semi-stable point bars. Fourth, additional flows from culverts may be influencing the meander geometry. Finally, the trajectory of a blown log revetment is considered. All stream photographs note the flow direction and within discussions the left bank and right bank refer to the left and right, respectively, when looking downstream.

### **Point bars**

Photography from 2004, when the revegetated floodplain plants were still young (Figure 34) illustrate that the point bar at the CS2 meander bend was not included in the revegetation plan. Additionally, the CS2 cut bank does not have revegetation growth. This is due to the fact that the bend apex was cut into the previous stream channel area in 2004 and was not included as part of the 2001 revegetation. This can be seen by comparing Figure 20B and Figure 20C at the two meander bends near the old channel.

Just upstream from CS2 was a channel bar in 2011 (Figure 35). The mid-channel bar had a split thalweg, and both left and right banks experienced undercutting. In 2013 and 2014 the mid channel bar became a sidebar with a backwater pool and the thalweg flow had completely migrated to the left bank, while still wetting the top of the bar (Figure 36). In 2007 the bar had looked as it did in 2013 and 2014, so the 2011 channel bar was intermediary. Additionally, photograhly from 2004 show that the flow was along the right bank with a point bar and side pool at the left bank. This adjustment over time shows a decrease in the radius of curvature of bend 4 at CS2.



Figure 33: 2013 photo looking upstream towards CS2.



Figure 34: 2004 same view of CS2 as previous figure showing the convex and cut banks both lacking the young willows visible in the right middleground. Photo courtesy of Matt Graul.



Figure 35: 2011 mid-channel bar with split thalweg at photo location "E", looking towards CS2. By 2013, the thalweg flowed against the left bank only, with backwater pools along the right bank.

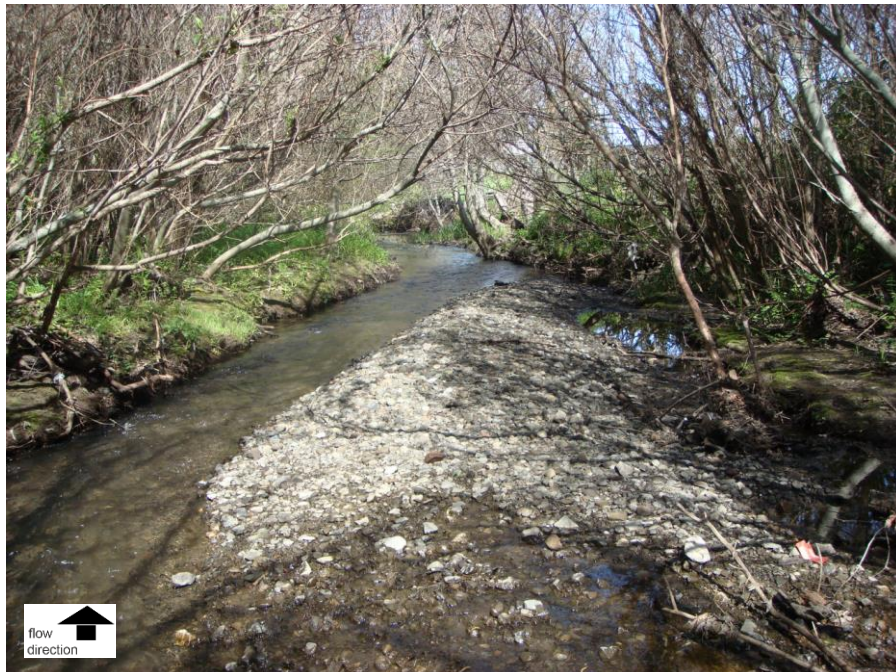


Figure 36: 2014 repeat photograph of location "E". The thalweg flows against the left bank. Right of the bar has filled in with coarse and fine sediment, while sustaining small side pools.

Unlike the other reaches with at least one point bar or channel bar, the stream reach between bend 5 and bend 6 had no bars or pools or riffles (Figure 37). This photo was taken from “I”, which is just upstream of the blown out log revetment at “G” in Figure 23. The waters in this reach were more like runs than riffles or pools. Additionally, the muddy banks have maintained the meander form seen in 2005 aerial imagery (Figure 20C), yet the 2004 imagery confirms that it was installed straight (Figure 20B).



Figure 37: 2013 meander form with muddy banks looking upstream from location “I”. Form maintained from the 2005 Figure 21B, into the 2011 LiDAR Figure 21A.

### **Secondary channel formation and chute cut-off**

The following series of photographs demonstrate the ongoing advancement of a chute cut-off at locations “A” and “B” from Figure 23. First, in 2007, there was a backwater eddy at an inflection point between design meander bends 1 and 2 (Figure 38). In 2007, field notes remark that the small backwater eddy had formed on a linear stretch of the stream, with a larger sediment size (cobble) bedform appearing bare of vegetation and continuing up the bank two meters. In 2011, the headcutting backwaters had continued up

another three meters, but still had no active flow (Figure 39). In both years, the thalweg flowed through the right bank channel (on the left in the photographs), which was deeper, faster, and narrower than other stream reaches in the study area.

Before 2007 the right bank had aggraded and the streambed channel had narrowed. This narrowed channel also aggraded slightly between 2007 and 2011, along with the longitudinal profile. In both years the left bank had thinner vegetation and sparse young willows, which is consistent with the lack of revegetation planned for the large design point bars. By 2013, the backwater formation at the inflection point had a slightly deeper eddy pool (Figure 40) and the cobbled bare ground continued up the same distance as in 2011.



Figure 38: 2007 backwater eddy and headcut located at "A". Main channel is along the right bank and the backwater eddy veers upstream on the left bank (lower right of photo).



Figure 39: 2011 Repeat photography of location "A" with a more defined headcut on the bank.



Figure 40: 2013 Repeat photography of location "A". Headcutting backwater has a slightly longer upstream pool length.

Further upstream from this secondary channel in 2007, the left bank Jubata grass blades were bent or broken forming a linear depression showing where water had flowed along the bank (Figure 41). Looking toward the left bank in 2007 from “B”, just upstream of the backwater channel, the trees are visibly distant from the stream showing the great size that the point bars were expected to grow to in the design (Figure 42). In the foreground, the Jubata grass is again lying flat. In 2011 this area looked similar to the 2007 images. However by 2014 the upstream area had headcut back into the main channel, establishing a small vegetated mid channel island (Figure 43). Further upstream a permutation of the side channel headcut extended up from the channel breach.



Figure 41: Upstream of “A” at location “B” in 2007 showing the invasive Jubata grass still folding down due to water flows (along right of photo).



Figure 42: Looking across to the left bank from the channel at “B” in 2007 shows vegetation downed by water and large trees planted far from the water’s edge.

This same upstream area was captured during the 2008 annual maximum daily precipitation event from January 25 (Figure 44). The chute cut-off channel adjustments could be explained by effective flows during peak discharge events. The storm return interval was between a 2.9 to 4.3 years (Table 3).

The processes influencing this chute cut-off is hypothesized to be: (1) Restoration revegetation excluded the designed overlarge meander bend convex side, which was expected to become a point bar, but did not and instead decreased bank stability; (2) The original channel along the right bank narrowed after a point bar successfully merged with the bank (discussed below); (3) Flood waters such as those in 2008 overflowed the banks and re-entered the channel at inflection points causing headcut erosion and a steeper channel parallel to original channel; and (4) This additional channel headcut up to the original channel, capturing some of the stream flow. As this process continues, the chute cut-offs will decrease stream sinuosity and increase the water surface slope.



Figure 43: 2013 photo looking upstream from location "B" showing chute cut-off upstream of "A".



Figure 44: 2008 repeat photograph from location "B" during a maximum daily precipitation event. The middle trees are the same as those in the middle background of Figure 43. Photo courtesy of Jerry Davis.

### **Lateral control adjustments**

Lateral controls in the reach include the log revetment footer logs on the cut-banks of the designed meanders, as well as the levee and earthen berm above the right bank, protecting residential and business areas. The footer logs are held in place by vertical logs or rootwads. These vertical logs stick up out of the bends and are clear indicators of the original as-built channel banks, even when footer logs are covered over with sediment.

There is evidence indicating that point bars are stabilizing and merging with banks, even where lateral controls are installed. For example, in Figure 45 and Figure 46, there are vertical rootwads visible behind banks and semi-permanent point bars. Figure 45 is located on the right bank at location “B”. This is where the channel narrowed and the left bank had the secondary channel with the successful chute cut-off, discussed above. This vertical log was just downstream of meander bend 2. Figure 46 is just downstream of meander bend 3 and was the last in a consistently spaced series of point bars starting near bend 4. Downstream of bend 4 near CS2 (not shown) there is a point bar in front of footer logs, but the footer logs are stacked taller into the terrace level.

Figure 47 and Figure 48 show photo location “H” (from Figure 23), which is upstream of meander bend 5 and not downstream like the other examples of vertical logs behind bars. There is a large point bar stretching more than halfway across the active channel, with exposed roots on the cut bank and the vertical log again indicating the original left bank back a meter behind the bar. Streamflow is wetting the top of the point bar. The photograph in Figure 49 was taken in late 2014 at the same location. The vertical log was captured during a late-2014 flood event and can be seen in the middle of the peak flood active channel.



Figure 45: Log revetments and vertical logs merged into the right bank at location "B".



Figure 46: Rootwad back up behind a point bar at location "C".



Figure 47: 2013 rootwad at location "H" indicates the original left bank, now behind a point bar.



Figure 48: Mid-2014 rootwad at location "H", from the left bank looking towards the stream.



Figure 49: Late-2014 rootwad (middle background) at location “H”, during a flood event. (Photo courtesy of Jerry Davis.)

### **Culverts**

The culvert draining into southeast of the restoration study area (Figure 50) discharges down an installed natural channel towards the creek (Figure 51). It then becomes shallower and dissipates into what appears to be a bioswale (Figure 52). The bioswale was either intentionally installed or is a function of the ditch ending and becoming shallow as it meets the dense revegetation on the floodplain before the stream. There is also a small hill mound located just north, contributing to the flow dissipation and bioswale impression. This channel can be seen in the lower right corner of the LiDAR in Figure 21A. The ditch had no flow during fieldwork days and a distinct confluence with the mainstem was not evident from the road or from the stream itself. However, it appears from the LiDAR data that the flow would meet the creek near “P”, just upstream of “H”, where the vertical log in Figure 47 is located.



Figure 50: “Culvert 1” drains under the decommissioned road at the lower right of the study area. The ditch continues along the road and ends before meeting the floodplain vegetation.



Figure 51: Looking up the ditch that drains from “culvert 1” into the study area. The ditch shows in the LIDAR elevation model (Figure 21A) coming in from the lower right corner.



Figure 52: The ditch draining "culvert 1" ends here in what may function as a bioswale.

There are at least two other drainage culverts opening into the study area from the decommissioned road to the south (Figure 53 and Figure 54). The first passes under the road near bend 5 and would carry flow from the steep incline to the south during storm events. The second opens into the study area from an unknown input location. Studying the natural channel meander process is complicated by the presence of these extra flow inputs, which could be influencing meander adjustments with both sediment and flow inputs.



Figure 53: A second culvert, “culvert 2”, draining under the decommissioned road into the floodplain area.



Figure 54: A third pipe, “culvert 3”, draining into the floodplain near the Highway 1 end of the decommissioned road.

### **The trajectory of a dislodged log revetment**

In 2013 the distinctive point bar in Figure 55 had been stable long enough for vegetation recruitment, shown in the foreground. In mid-2014, the bar was still well-defined with a woody debris being used as a footbridge across the active channel (at left in Figure 56). The 2013 thalweg is pushed against the cut bank, undercutting the right bank trees and exposing roots. This is beneficial for steelhead trout, as undercut banks and woody debris both contribute to beneficial pools where they can rest and hide. Figure 57 shows the same point bar, but looking downstream, where the advancement of the bank vegetation is visible. There is a slight indentation along the left bank (at right) where peak flows carved between the infilling bar and the prior channel bank (similar to Figure 47). But then in Figure 58, taken after a flood event in late-2014, a dislocated log revetment had arrived and settled into the nook on the point bar. The log was also already undercutting.

The out-of-place log revetment lying along the left bank in Figure 58 looks like it could possibly be part of the bank stabilization. This is especially true because it landed along the bank of the active channel. However, it is not located at a design meander bend, where the footer logs were installed. Additionally, its trajectory was documented showing that it arrived here in late 2014 after moving from bend 5 upstream, where it was seen between 2007 and early 2014. It is hypothesized that its original placement was upstream of bend 5, along the left bank. However, documentary photography in 2004, when the revetments were installed, do not show the assumed log location clearly, and therefore it is not definitive. Additionally, one of the the Lee (1999) design sketches for the restoration shows log jams installed at each meander bend. It is possible the log crossing the stream at bend 5 before late 2014 was intentionally installed there. However, it is unlikely, as documentary photography from 2004 shows that other meander bends do not have log jams installed. Therefore, this design element was probably not implemented.



Figure 55: A cobble and pebble bar in early 2013 at location “F”. Vegetation has colonized the bar in the foreground. A relatively uniform particle size overlays a heterogeneous bedload. The thalweg undercuts the right bank and exposes tree roots.



Figure 56: August 2014 point bar at location “F”, looking upstream.



Figure 57: March 2013 point bar at location “F”, looking downstream.



Figure 58: December 2014 point bar at location “F” recruits a large blown out log revetment after a storm event. The blown-out log revetment has settled into the bar and is already developing an undercut. Photo courtesy of Jerry Davis.

Before 2007 the large log was most likely a left bank footer log along bend 5 near location “I” (locations illustrated in Figure 23). In 2007 it was found completely blocking the channel, crossing almost perpendicularly and creating a trash and debris dam at location “G” (Figure 59). Before the fall 2011 fieldwork, the log had repositioned at bend 5 pointing slightly downstream. This unblocked the trash dam (Figure 60). Between 2007 and 2011, the 2008 annual maximum daily precipitation event was photographed (Figure 61) showing the trash dam still present. The 2011 repositioned log at bend 5 is shown in Figure 62 to be opened up slightly pointing downstream.

In mid-2014, the log was in the same position as it was in 2011. However, in late 2014, a flood event transported the log across the channel to the left bank behind the riparian vegetation (Figure 63). After the floodwaters receded, it can be seen resting on the side bar (Figure 58) discussed above.

Although USACE expects that the revetments and other restoration and flood management controls will be monitored and maintained by the City of Pacifica, this log revetment has had an unimpeded and independent trajectory. In 2007, this revetment created the deepest pool in the reach. By 2011, that same log had opened up downstream, clearing out the trash and aggrading the scour pool slightly. In a natural system, such increased complexity would be beneficial for steelhead. But with upstream areas adding pollution to the system, trash can be trapped by woody debris, even during peak storm events, such as in 2008. Now the log is positioned along a convex bend (location “F”) of a smaller meander wavelength meander within the larger designed meander wavelength. It is unknown whether this increased complexity and compromise of the original revetment affects the flood protection achieved by the restoration.



Figure 59: 2007 blown log revetment at location “G” spans the width of the stream, trapping trash and debris and causing a deep scour pool beneath it.



Figure 60: Blown out revetment at “G” opened up downstream by 2011 extending only halfway across the width of the stream, clearing the debris and reducing the scour pool depth.



Figure 61: Early 2008 flood event shows the blown revetment at location "G". Note the rootwad in the lower left foreground, also in other photos in this series. Photo courtesy of Jerry Davis.

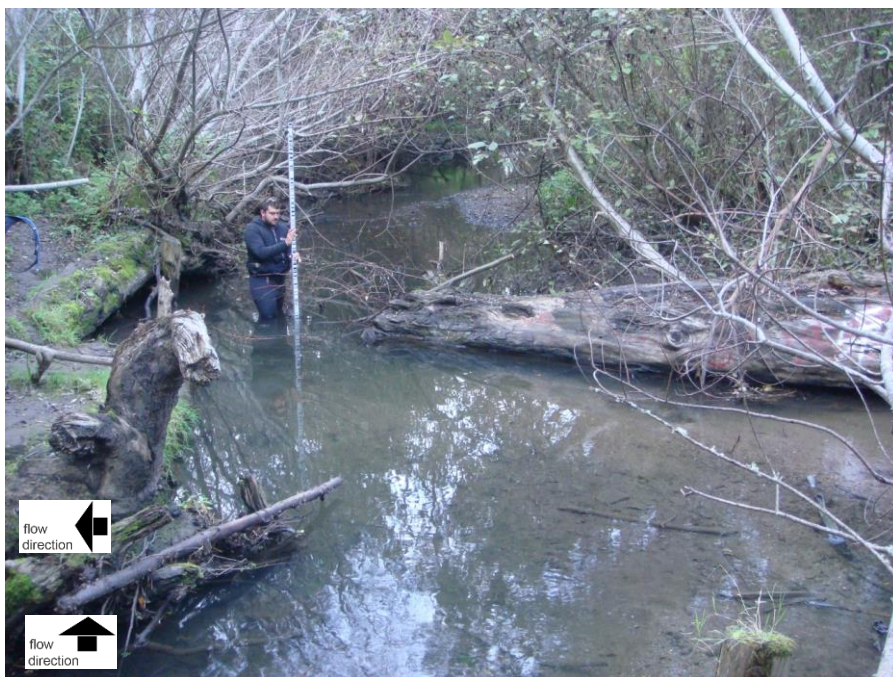


Figure 62: Looking downstream at the revetment at location "G" in 2011. In 2007, there was no gap between the left bank and the blown out log revetment across the stream.



Figure 63: Late 2014 flood event shows the blown out log revetment at location “F” (also shown in Figure 58 after the waters recede). It was transported from location “H”. Photo courtesy of Jerry Davis.

A possible explanation for the trajectory of the moving log is that flashy discharge from culvert 1 originally dislodged the footer log and contributed to its further advance (Figure 64). The dry ditch draining culvert 1 is not visible in 2002 or 2005 orthoimagery, but is apparent in 2011 (Figure 64 left images). Therefore by at least 2011, the channel lacked permanent vegetation and thus had regular flow. The planview sketch detail shows the culvert 1 flow direction and bioswale mound, while the 2011 LiDAR imagery clearly shows that the ditch narrows and turns downstream before it reaches the stream channel. So, the flow from the culvert could be high enough, while also entering the stream from behind the log, to blow the log out of its original position (pre-2007) and continue to move it downstream during peak flow events.

Flows from this culvert could also explain the increase in point bars downstream of bend 5 versus upstream, if the flows carry a high sediment load. The difference might be

explained by a deficit of sediment supply due to long-term culverting of the North Fork contrasting additional sediment inputs from culvert 1. Peak flows from culvert 1 may also explain the rapid meander formation on this reach. In 2002 (Figure 64) and in 2004 (not shown), there was no distinct finer scale meander. But then the 2005 imagery (Figure 64) shows the meander formed less than a year after flow was established in the new channel.

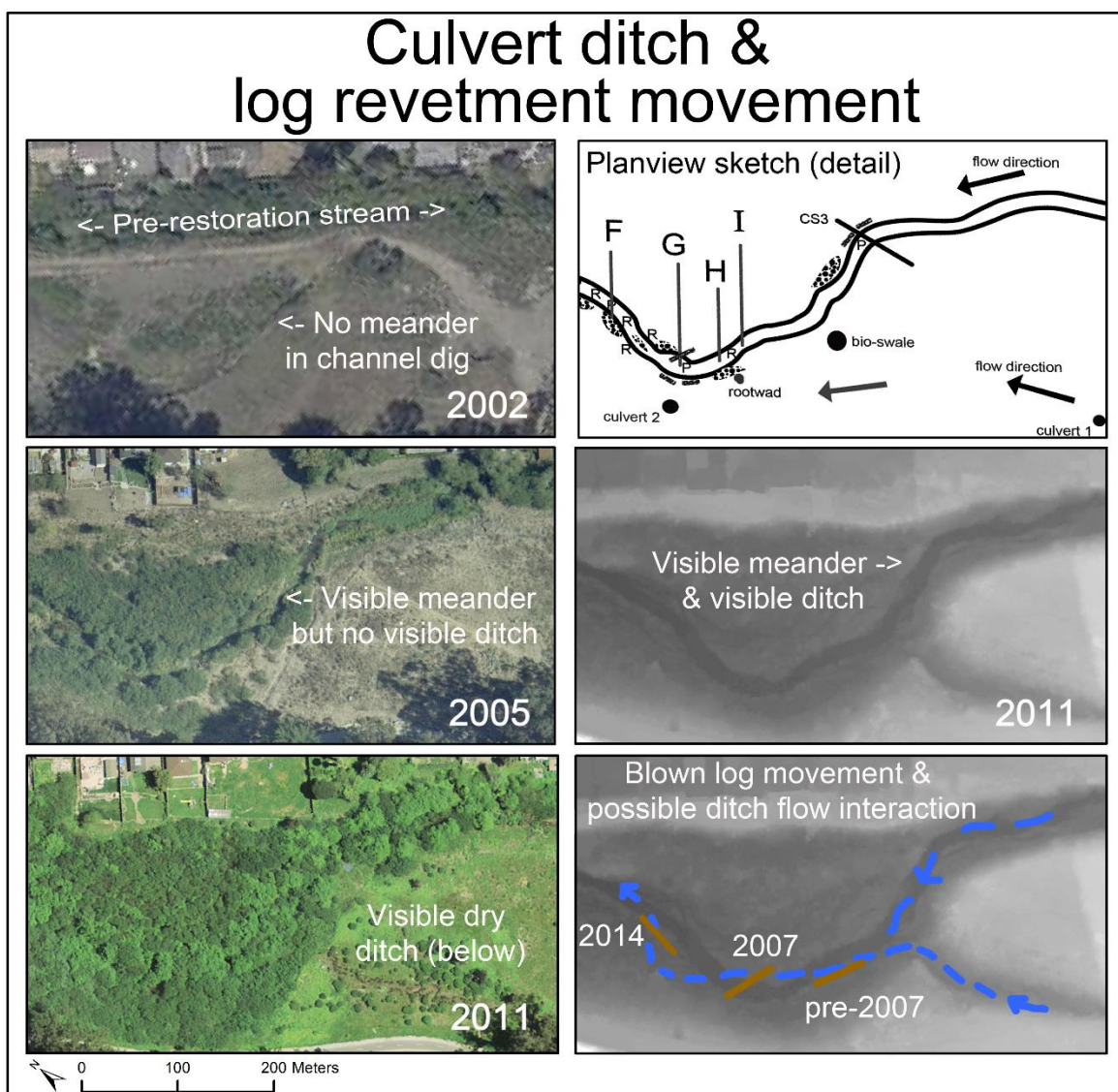


Figure 64: Hypothesis for the log movement (brown) and culvert flow (blue) over time.

### **Anthropogenic influences**

Trash accumulation is a problem on the site. The Highway 1 Bridge at the downstream end of the study area amassed trash dams seen on many fieldwork days. During the 2008 annual maximum daily precipitation event, there was no trash at the Highway 1 Bridge (Figure 65) because the trash was trapped behind the log revetment upstream at location “G” (Figure 59). However, the log repositioned by 2011 (Figure 60 and Figure 62) and the trash dam relocated downstream to the bridge, trapped by small woody debris (Figure 66). In 2014, there were two additional trash dams on the reach trapped behind small instream woody debris piles, while the bridge trash dam was gone due to the bridge construction project (Figure 67).



Figure 65: 2008 peak flood event, looking downstream at the Highway 1 Bridge. There is no garbage/debris accumulation here. Photo courtesy of Jerry Davis.



Figure 66: Looking downstream at the Highway 1 Bridge in 2013, with more overhanging vegetation – and a lot more trash blocked by woody debris.



Figure 67: The Highway 1 Bridge was removed in 2014 and no longer had a trash dam. Traffic is shown re-routed over another adjacent bridge just downstream during reconstruction.

Other anthropogenic influences on the stream reach are residential landscaping and homeless encampments. At CS2 a streamside neighbor was landscaping the earthen berm easement with native *Juncus* and brick walkways (Figure 68). On each fieldwork day, homeless encampments were visible within the dense vegetation and were accompanied by trash piles.



Figure 68: Homeowner landscaping with *Juncus* along the easement terrace at CS2. Sprinkler in foreground is part of CS2, and is a remnant of the now inactive revegetation watering system.

In 2013, a streamside encampment (Figure 69) appeared between bend 3 and bend 4, which has easy access to the decommissioned road through the trees. There were three large piles of garbage around the tent and pots and pans were on a point bar in the stream.



Figure 69: Homeless encampment near CS1. Cooking utensils are on the channel bar and the camp is surrounded by trash piles.

Landscaping and camping in the stream reach are not inherently hazardous to the geomorphology and ecology of the reach. However, more research is needed on the effects of regrading, vegetation modifications, and additional garbage inputs on stream habitat and flood hazard.

## DISCUSSION

A stream restoration project in coastal California integrated ecological restoration with flood control on the 500 m floodplain reach draining the 21 km<sup>2</sup> San Pedro Creek Watershed in Pacifica, California. Fieldwork, LiDAR data, and repeat photography were compared with planning documents, flood modeling, and aerial imagery, allowing identification of processes acting to destabilize the reach and produce unexpected morphologies. The following sections discuss key findings with respect to stream geomorphology and levels of flood protection achieved by the restoration project, as well as considerations for future research.

### **Longitudinal profiles, cross-sections, and lateral controls**

USACE and stream restoration designers used lateral controls for the San Pedro Creek restoration project in order to stabilize the active channel in an urbanized area with limited land available for a floodplain. The project included an active channel meander constrained with footer logs and vertical logs to minimize channel migration, as well as a natural levee and berm on the right bank to protect residential and business areas. For the period 2003 to 2011, the aggradation and degradation trends in parts of the longitudinal profile alternate, suggesting an oscillation towards an equilibrium. Additionally, two of the three cross-sections show no streambed elevation change, while the third shows an apparent oscillation in bed elevation. This also suggests a stability in the reach.

Identifying natural meander adjustment processes are more difficult in a reach with restoration-installed lateral migration controls such as log revetments. Nevertheless, including them in the assessment of meander adjustments could provide important information on restoration outcomes and stability given artificial lateral controls in urban areas with restricted floodplain availability.

Repeat documentary photography reveals that the active channel has migrated away from at least three footer logs, depositing point bars in front of them, and one log revetment has blown out and relocated downstream. Additionally, one successful chute cut-off has occurred. These suggest that either the reach is still adjusting and has not yet reached a stable equilibrium or that these types of changes will be part of the equilibrium. Nevertheless, the lateral controls are functioning reasonably well to slow meander adjustments, while also providing valuable fish habitat.

The intermittent flow from the culvert ditch may explain the blown out log revetment, which probably originated along the left bank of the stretch with no point bars between bend 5 and bend 6. During peak flood events, the extra flow from the culvert could be responsible for moving the footer log. Additionally, it could potentially contribute sediment from the very steep 0.4 km<sup>2</sup> subwatershed draining into the culvert from Pedro Point Headlands, which has a history of erosion due to recreational activities. An increased sediment load at the confluence, along with a deficient load coming from the culverted North Fork, could help explain an increase in point bar frequency downstream.

### **Restoration design and meander adjustments**

Documentary photographs of the stream reach contributed to the interpretation of the geomorphic processes over time. Some of the main points gathered from them are:

- (1) Point bar deposits are initiating smaller wavelength meander formation within linear reaches by forcing thalweg lateral migration, undercutting opposite banks, and infilling sand and pebble point bars with silts and clays. The resultant radius of curvature is also smaller, but the bankfull width is maintained.
- (2) Channel bars with split thalwegs are widening the active channel width as part of meander wavelength and radius of curvature adjustments.
- (3) Side channel formation, with potential to initiate chute cut-off, is preceded by headcut eroding backwaters up from designed meander inflection points.

(4) Meander adjustments on the reach are towards smaller meanders with more frequent bedforms than the initial planned meander.

The primary weakness of the restoration design was the unsuitable meander geometry. Particularly, the meander wavelength and radius of curvature relative to the active channel width and stream discharge did not account for realistic point bar spacing. Four of the linear reaches between the five design meanders have developed established point bars with scale-appropriate spacing, which are shown by linear models to be natural triggers of channel alignment changes (Pittaluga and Seminara 2011). A channel originating with a uniform bedform width, such as the SPC restoration, experiences first secondary flow-caused formation of mid-channel bars, which is followed by channel widths variations, and further meander migration forced by the channel width variations. In SPC, this results in a bimodal meander because the point bar patterns are at a smaller wavelength than the larger design meander wavelength.

Because the stream design left space for large point bar development on the convex bank of meander bends that were ultimately too large relative to the watershed size, those areas did not develop point bars. Thus the bare soil became a recruitment area for both the nearby revegetated natives, as well as local invasive varieties like Jubata grass. When streamflow was routed into the restoration reach in 2004, new vegetation in the bare areas was less mature than the revegetated areas. The structural weakness of inflection points in streams built to overbank frequently stems from the fact that this is precisely where overbank flow would be reentering the active channel during storm events. The convex bank erodes at the inflection point as the overbank flow reenters the active channel. In SPC, the inflection point erodibility is compounded by the fact that the convex banks of the designed meander bends were omitted from the revegetation scheme. The lack of bank stabilizing vegetation at inflection points allowed headcut erosion and initiated the development of the chute cut-off upstream of CS1. The restoration design projected

longitudinal profile and cross-section monitoring twice per year (Lee 1999) in order to identify maintenance requirement that would stabilize the active meander channel. However, there has not been such a monitoring program, and therefore the channel is adjusting in interesting ways without human interventions.

The LiDAR data were found to supplement and improve geomorphologic assessment based on fieldwork data, particularly in estimating the actual radius of curvature of the evolving meander geometry as compared to the designed meander geometry. Breaklines from the DTM showed a radius of curvature of 20 m. This is almost equal to the Davis (2008) theoretical value of 20.7, but far lower than the Lee (1995) Rosgen planning document value of 38.1 m, the Lee (1995) planview drawings illustrate a value of 45 m, and the as-built measures a value of 62 m. The DTM also helped identify the development of side channels and other micro-features. It was not functional for longitudinal profile generation, because it did not penetrate the water surface – and the derived stream channel was too noisy at that high of resolution to be meaningful.

### **Flood model**

Although the flood model showed levee and berm overtopping at 50- and 100-year flood levels for the as-is bridge, and at 100-year levels for the proposed new bridge, there are some limitations to the accuracy and interpretation of the model. Primarily, the narrow cross-sections make interpreting the flood hazard to the south for 50- and 100-year floods with the as-is or proposed new bridge difficult to gauge. The preliminary HEC-RAS model shows overtopping of levees and reaching left bank model extents, but it does not show where the full extent of the flooding would occur because the model is limited to a narrow band around the stream reach. The band ends just after the levee to the north and just before the steep rise to the south.

Additionally, the bridge re-design only improved the flood model outcomes slightly. Fortunately, the Highway 1 Bridge cross-sections do not overtop at the 100-year level with the proposed bridge. However, the 100-year level still does overtop at CS2 and along the left bank. Including the as-built dimensions of the new bridge after it is completed in 2015 will make the model more accurate.

One improvement to the model was found in USACE's increase of both instream and floodplain Manning's n values, as compared to the design Manning's n proposed by Lee (USACE 2013). The higher values are more appropriate given the increase in roughness, as compared with the initial installation before revegetation. There is now dense vegetation on the floodplain, overhanging vegetation on the banks, and the presence of woody debris and trash in the stream.

### **Considerations for future research**

San Pedro Creek provides an important case study of fixed-form design with process-invoked channel changes. Future research opportunities include wider and repeated cross-section, modeling the extent of flooding, point-bar spacing and sediment supply analysis, monitoring chute cut-off progression and meander changes, and stream gauge installation with special attention to correlating it with historical daily precipitation data. Lee (1999), expected staff and crest gauges to be installed up and downstream of the reach in order to calibrate flood events with bankfull indicators as well.

The three cross-sections in this study do not adequately represent the pool-riffle sequences in the stream reach and therefore future research and monitoring including a variety of cross-sections would improve understanding and prediction of the stability on the reach. The protocol could involve repeating the contractor cross-sections, which focused on revetted bend apices and are repeatable, or selecting relevant cross-sections to survey such as at riffles and pools, point bars, stable revetments, and setback vertical

logs. In addition, extending the cross-sections uphill to the south and into the residential area to the north (using surface models or fieldwork) would allow for modeling flood extent within HEC-RAS.

More research is needed on the sediment supply and discharge volumes from the mainstem, as well as from the culverts and the hillslope to the south of the study area. This would guide effective modifications for avoiding another log revetment blow out, while also informing theoretical models for designing point bar spacing and pool-riffle spacing in natural urban streams with lateral controls.

The head-cutting chute cut-offs reveal the process of flood waters re-entering the active channel at inflections points and causing headcut erosion there. This, along with the rootwads behind the stable channel bars, provide visible clues that the designed form is adjusting due to the point bar meander geometry variable errors. Observing and measuring these changes over time would inform future urban stream restoration design.

There was a general disconnect between geomorphology theory and civic implementation of the stream restoration, which was inexpertly based on Rosgen natural stream design. The Lee (1995, 1999) designs were based on ecosystem function forms and not necessarily geomorphological processes. Additionally, the union of urban stream restoration with flood control relied upon lateral controls not accounted for in geomorphologic stream variables describing natural systems. Therefore, further research is needed on urban stream restoration in particular, and the possible appropriate variations of form and process within urbanized areas.

## CONCLUSIONS

This case study examined the results of a federal flood control project on San Pedro Creek in Pacifica, California that integrated ecological stream restoration principles with traditional engineering flood control methods. In order to understand the effects of the restoration efforts on the creek, field research was conducted to assess the geomorphology of the restored reach and included cross-sections, longitudinal profiles, and pebble counts. Digital terrain models and site photography, as well as planning documents and a hydrologic flood model obtained from USACE, supplemented the data collected in the field in order to evaluate the changes in the meander planview as compared to the designed channel, to note evidence relating to stability or equilibrium, and to gauge the level of flood control achieved.

It was found that the planview has changed in two significant ways. First, three rootwads were found in 2011 to be up on the bank, behind semi-permanent point bars. The point bar deposition, obfuscating the previous bank and separating the lateral control from the active channel, all three appeared just downstream of a meander bend. This signals a channel adjustment lowering the radius of curvature and the meander wavelength. Second, the development of a secondary channel was found in 2013 adjacent to the main channel, connecting to the main channel both up and downstream. This side channel was seen in 2007 as an initiation of a chute cut-off starting at the inflection point downstream of a bend, and headcutting up on the bank through 2011 and 2013. This signals the creation of a small channel island, along with the potential for further headcutting that could either capture the main channel flows further upstream or else fill in over time. The chute cut-off stems from the lack of bank stabilizing vegetation in the design of the large meander bends, as well as a lack of monitoring and repair of the installed meander over the course of ten years. Ultimately, these channel changes signify a potential for flood hazard due to a loss of lateral control, although more research is needed to confirm this.

Within an 8-year period, an equilibrium was suggested in the longitudinal profiles. The reach experienced net aggradation (2003–2005) followed by degradation (2005–2007) and then aggradation (2007–2011), resulting in an elevation and slope profile in 2011 similar to that of 2003. However, the lateral geometry appears to be generating finer scale reach evolutions within the larger meander, increasing sinuosity. At the same time, a chute cut-off formed in 2014, which decreases the sinuosity. These sinuosity adjustments may be part of an oscillation around an equilibrium sinuosity. Further monitoring is necessary to reach the determination of equilibrium.

Finally, results from the hydrologic flood model indicate that a 100-year flood protection level was not achieved as a result of the restoration project. The preliminary HEC-RAS model provided by the USACE shows at least a 25-year flood return interval protection. However, it also indicates 50- and 100-year flood return interval breaches at the pre-restoration bridge downstream of the reach and along a meander bend adjacent to a residential area. The new bridge will be completed in 2015, but the model still shows breaches at the 100-year level. The Manning's  $n$  values used in this flood model were modified from and more appropriate for the now thickly vegetated banks than the original design Manning's  $n$  values. However, the flood model was restricted by a narrow model extent and a preliminary design of the new bridge. Therefore further cross-section research and modeling is required to fully determine the accuracy of the model and extent of potential flooding.

This reach of San Pedro Creek serves as a laboratory for assessing ecological stream restoration goals alongside flood control effectiveness. For now, the resultant geomorphology, with undercut banks recruiting woody debris, creates more suitable habitat for steelhead than existed in the channel before the restoration. Additionally, the

development of chute cut-offs can create backwater pools at low flow suitable for California red-legged frog habitat.

Both flood control and stream restoration are human interventions with natural processes. Due to environmental regulations, further integration of ecological concerns with flood control will continue to become more commonplace. However, merging the two objectives of flood control and ecological stream restoration did not result in a theoretically accurate geomorphological plan in the case of San Pedro Creek. In fact, varying and overlarge values for the meander wavelength and the radius of curvature suggest the benefit geomorphologists could bring to the design plan, given their familiarity with geomorphological processes creating stream forms. Including geomorphologists in the collaboration between ecologists and engineers could potentially contribute to a more sustainable final stream restoration and flood control design. However, monitoring and maintenance would likely still be recommended due to the potential hazards to urban populations. It is still unclear if the softer path solutions can provide adequate flood protection, although it is clear, based on observations along the stream reach, that ecological restoration is a benefit even in this small area, with a good frequency of pool and riffle habitats and ample shade from vegetation. Finally, urban stream design includes development constraints not integrated into natural stream design and further study is needed to classify and design urban stream restoration and flood control projects that use lateral controls.

## REFERENCES

- Amato, P. F. 2003. *Effects of urbanization on storm response in the North Fork San Pedro Creek*. Unpublished San Francisco State University Master of Arts Geography thesis.
- Brabb, E. E., R. W. Graymer, and D. L. Jones. 1998. *Geology of the Onshore Part of San Mateo County, California: Derived From the Digital Database Open-File 98-137*. Retrieved 2014 from: <http://pubs.usgs.gov/of/1998/of98-137/>
- Brabb E. E., E. H. Pampeyan, and M. G. Bonilla. 1972. *Landslide susceptibility in San Mateo County, California scale 1:62500*. Miscellaneous Field Studies Map MF-360. Washington, DC, USA.
- Braudrick, C. A., W. E. Dietrich, G. T. Leverich, and L. S. Sklar. 2009. Experimental evidence for the conditions necessary to sustain meandering in coarse-bedded rivers. *Proceedings of the National Academy of Sciences*, 106(40), 16936-16941.
- Collins, L. 2001. *San Pedro Creek Watershed Pilot Assessment*. San Mateo: San Mateo Countywide Stormwater Pollution Prevention Program.
- Collins, L., P. Amato, and D. Morton. 2001. *San Pedro Creek Geomorphic Analysis*. Report funded by the San Francisco Bay Regional Quality Control Board through the San Pedro Creek Watershed Coalition.
- Collins, L. and R. Leventhal. 2013. *Regional Curves of Hydraulic Geometry for Wadeable Streams in Marin and Sonoma Counties, San Francisco Bay Area Data*

*Summary Report*. Retrieved 2014 from: <http://www.sfestuary.org/wp-content/uploads/2014/05/Stream-Design-Curve-Marin-Sonoma-2013.pdf>

CP (City of Pacifica) and USACE (U.S. Army Corps of Engineers). 1998. San Pedro Creek Section 205 Flood Control Study, Final Detailed Project Report, Vol. II, Technical Appendices.

Culp, J. 2002. *Landscape of San Pedro Valley, Pacifica, California*. Unpublished San Francisco State University Master of Arts Geography thesis.

Davis, J. 2008, April. *Fluvial geomorphic adjustments in a flood control / wetland restoration project*. Paper presented at the meeting of the Association of American Geographers, Boston, MA.

Davis, J. D., and S. M. Sims. 2013. Physical and maximum entropy models applied to inventories of hillslope sediment sources. *Journal of Soils and Sediments* 13.10 (2013): 1784-1801.

Davis, J., S. Sims, S. Pearce, L. McKee, S. Shonkoff, and S. Holmes. 2004. *San Pedro Creek Watershed Sediment Source Analysis*. San Francisco State University.

Dunne, T., and L. Leopold. 1978. *Water in Environmental Planning*. New York: W.H. Freeman and Company. Drainage area curve available here: <http://www.sfestuary.org/wp-content/uploads/2014/05/Original-Design-Curves-Dunne-and-Leopold-1978.pdf>

Gay, G. R., H. H. Gay, W. H. Gay, H. A. Martinson, R. H. Meade, J. A. and Moody. 1998. Evolution of cutoffs across meander necks in Powder River, Montana, USA. *Earth Surface Processes and Landforms*, 23(7), 651-662.

Groundspeak. 2015. *Details for Benchmark: HT1823*. Retrieved 2015 from <http://www.geocaching.com/mark/details.aspx?PID=HT1823>.

Hooke, J. 2003. River meander behaviour and instability: a framework for analysis. *Transactions of the Institute of British Geographers* 28 (2):238-253.

Ivanetich, K. M., P. H. Hsu, K. M. Wunderlich, E. Messenger, W. G. Walkup IV, T. M. Scott, J. Lukasik, and J. Davis. 2006. Microbial source tracking by DNA sequence analysis of the *Escherichia coli* malate dehydrogenase gene. *Journal of Microbiological Methods*, 67(3), 507-526.

Johnson, R. M. 2005. *A Basin-Wide Snorkel Survey of the San Pedro Creek Steelhead (Oncorhynchus mykiss) Population*. Unpublished San Francisco State University Master of Arts Geography thesis.

Jurmu, M. C. 2002. A morphological comparison of narrow, low-gradient streams traversing wetland environments to alluvial streams. *Environmental management* 30 (6):0831-0856.

Keller, E. A. 1972. Development of alluvial stream channels: a five-stage model. *Geological Society of America Bulletin* 83 (5):1531-1536.

Knighton, A. D. 1977. The meander problem. *Geography*, 106-111.

Kondolf, G. M. 1998. Lessons learned from river restoration projects in California. *Aquatic Conservation: Marine and Freshwater Ecosystems* 8 (1):39-52.

Kondolf, G. M., 2000. Assessing salmonid spawning gravel quality. *Transactions of the American Fisheries Society*, v. 129, p. 262-281. As cited in Pearce, McKee, and Shonkoff (2004).

Kondolf, G. M., S. Anderson, R. Lave, L Pagano, A. Merenlender, and E. S. Bernhardt. 2007. Two decades of river restoration in California: what can we learn? *Restoration Ecology* 15 (3) 516-523.

Lee (L.C. Lee and Associates, Inc.). 1995. *Report to the City of Pacifica on the 75% Design for Resorting Lower San Pedro Creek and Adjacent Wetlands*. Pacifica, California: Prepared for Mr. Scott Holmes, Wastewater Program Manager.

———. 1999. *Final Monitoring Plan for the Restoration of the Lower San Pedro Creek Ecosystem*. San Francisco, CA.

Leopold, L. B., and G. M. Wolman. 1960. River meanders. *Geological Society of America Bulletin*, 71(6), 769-793. As cited by Williams 1986.

Leopold, L. B., G. M. Wolman, and J. B. Miller. 1964. *Fluvial Processes in Geomorphology*. San Francisco: W. F. Freeman and Company.

Luchi, R., G. Zolezzi, and M. Tubino. 2010. Modelling mid-channel bars in meandering channels. *Earth Surface Processes and Landforms* 35 (8):902-917.

McDonald, K. N. 2004. *San Pedro Creek Flood Control Project: Integrative Analysis of Natural Hazard Response*. Unpublished San Francisco State University Master of Arts Geography thesis.

Parsons, T., J. McCarthy, P. E. Hart, J. A. Hole, J. Childs, D. H. Oppenheimer, and M. L. Zoback. 2002. A review of faults and crustal structure in the San Francisco Bay Area as revealed by seismic studies: 1991-97. *US Geological Survey professional paper*, (1658), 119-145.

Pearce, S.A., L. J. McKee, and S. B. Shonkoff. 2004. San Pedro Creek Watershed Sediment Source Analysis, Volume III: Tributary sediment source assessment. *In*: Davis, J., 2004. *San Pedro Creek Watershed Sediment Source Analysis*. A report prepared for the City of Pacifica, California and San Francisco Estuary Institute Contribution #87.

Pittaluga, M. B., and G. Seminara. 2011. Nonlinearity and unsteadiness in river meandering: a review of progress in theory and modelling. *Earth Surface Processes and Landforms* 36 (1):20-38.

Riley, Ann. 2002. *A Primer on Stream and River Protection for the Regulator and Program Manager*. Technical Reference Circular W.D. 02-#1. San Francisco: San Francisco Bay Region California State Water Quality Control Board. As cited by Davis (2008).

Rosgen, D. L. 1994. A classification of natural rivers. *Catena* 22 (3):169-199.

Rutherford, I. D. 1994. Inherited controls on the form of a large, low energy river: The Murray River, Australia in Schumm, S. A. and B. R. Winkley, eds, *The Variability of the Large Alluvial Rivers*. New York: ASCE Press. 177-197. As cited by Hooke (2003).

San Francisco Estuary Partnership. 2014. *Stream Restoration Design Curves*. Retrieved 2014 from <http://www.sfestuary.org/designcurve>.

Sassoubre, L. M., S. P. Walters, T. L. Russell, and A. B. Boehm. 2011. Sources and fate of Salmonella and fecal indicator bacteria in an urban creek. *Journal of Environmental Monitoring*, 13(8), 2206-2212.

Small Flood Control Project Authority. 1976. 33 C.F.R. § 263.23 Section 205. Retrieved 2014 from: <http://www.law.cornell.edu/cfr/text/33/263.23>

SPCWC (San Pedro Creek Watershed Coalition). 2002. *San Pedro Creek Watershed Assessment and Enhancement Plan*. Prepared for the California Department of Fish and Game.

Stoffer, P. W. 2006. *Where's the San Andreas Fault?: A Guidebook to Tracing the Fault on Public Lands in the San Francisco Bay Region* (Vol. 16). US Geological Survey. Retrieved 2014 from: <http://pubs.usgs.gov/gip/2006/16/>

Towill. 2011. *Survey of Downstream Reach, Pacifica, CA*. San Francisco: Report for USACE SF District, Civil Design Section.

TRA Environmental Sciences. 2007. *San Pedro Creek Ecosystem Restoration Program 2007 Compliance Monitoring Report*. Pacifica, CA: Prepared for City of Pacifica.

Ungvarsky, K. 2002. Draft report: A Cultural Resources Study and Discovery Report for the San Pedro Creek Flood Control and Wetland Restoration Project, City of Pacifica,

San Mateo County, California. Prepared for USACE SF District. Internship project 50001-2000, student of Anthropological Studies Center, Sonoma State University.

USACE (U.S. Army Corps of Engineers). 1998. *Section 205 Detailed Project Report for Flood Control: San Pedro Creek, City of Pacifica, California.*

USACE (U.S. Army Corps of Engineers). 2013. *HEC-RAS Preliminary Flood Model for San Pedro Creek.*

USACE (U.S. Army Corps of Engineers). 2014. *San Pedro Creek, Pacifica, Sec. 205.*

Retrieved 2014 from:

<http://www.spn.usace.army.mil/Missions/ProjectsandPrograms/ProjectsbyCategory/ProjectsforFloodRiskManagement/SanPedroCreek,Pacifica,Sec205.aspx>

USACE (U.S. Army Corps of Engineers) and CP (City of Pacifica). 1998. *Final Environmental Impact Report/Environmental Impact Statement: San Pedro Creek Flood Control Project.* State Clearinghouse Number: 95083039.

Viglione, A., R. Merz, and G. Blöschl. 2009. On the role of the runoff coefficient in the mapping of rainfall to flood return periods. *Hydrology and Earth System Sciences*, 13(5), 577-593.

Wagner, T. P. 1976. *Testing a field level approach for Corps of Engineers water resources planning.* Unpublished Stanford Doctoral thesis.

Weiss, S., A. Flint, L. Flint, D. Ackerly, and E. Micheli. 2013. *High resolution climate-hydrology scenarios for San Francisco's Bay Area.* A final report prepared by the Dwight

Center for Conservation Science at Pepperwood, Santa Rosa, CA, for the Gordon and Betty Moore Foundation.

Wilcock, P. R. 2012. Stream Restoration in Gravel-Bed Rivers. In *Gravel-Bed Rivers: Processes, Tools, Environments, 2<sup>nd</sup> edition*, 137-149. Hoboken, NJ: Wiley.

Williams, G. P. 1986. River meanders and channel size. *Journal of hydrology*, 88(1), 147-164.